

Exploring the electromagnetic properties of the $\Xi_c^{(\prime,*)}\bar{D}_s^*$ and $\Omega_c^{(*)}\bar{D}_s^*$ molecular states

Fu-Lai Wang^{1,2,3,*}, Si-Qiang Luo^{1,2,3,†}, Hong-Yan Zhou^{1,2,‡}, Zhan-Wei Liu^{1,2,3,§} and Xiang Liu^{1,2,3,¶}

¹*School of Physical Science and Technology, Lanzhou University, Lanzhou 730000, China*

²*Research Center for Hadron and CSR Physics, Lanzhou University and Institute of Modern Physics of CAS, Lanzhou 730000, China*

³*Lanzhou Center for Theoretical Physics, Key Laboratory of Theoretical Physics of Gansu Province, and Frontiers Science Center for Rare Isotopes, Lanzhou University, Lanzhou 730000, China*

In this paper, we systematically study the electromagnetic properties, including the magnetic moments, the transition magnetic moments, and the radiative decay behavior, of the $\Xi_c^{(\prime,*)}\bar{D}_s^*$ -type hidden-charm molecular pentaquarks with double strangeness and the $\Omega_c^{(*)}\bar{D}_s^*$ -type hidden-charm molecular pentaquarks with triple strangeness. Some effects such as the S - D wave mixing effect and the coupled channel effect are considered when discussing their electromagnetic properties. The present studies around the electromagnetic properties of hidden-charm molecular pentaquarks with double or triple strangeness are all part of a continuum of spectroscopic behavior of the hidden-charm molecular pentaquarks.

I. INTRODUCTION

As the academic frontier of hadron physics, the study of the exotic hadronic states has been a hot spot focused by both theorists and experimentalists over the past two decades [1–22], since exotic hadronic states are beyond the conventional meson ($q\bar{q}$) and baryon (qqq), which may construct new particle zoo. In fact, it is not limited to the construction of the exotic hadron family. The study of exotic hadronic states may also provide unique insights to deepen our understanding of the non-perturbative behavior of the strong interactions.

Among the various assignments of exotic hadrons to these observed new hadronic states, the molecular state explanation is popular because of the existence of corresponding thresholds of two hadrons close to some observed new hadronic states. It makes the hadronic molecular states to be extensively studied in the last 20 years [1–22]. In particular, after observing two P_c states in 2015 [23], the LHCb Collaboration reported two substructures, the $P_c(4440)$ and $P_c(4457)$, corresponding to the previously observed $P_c(4450)$ [23], and found a new $P_c(4312)$, where LHCb again analyzed the $\Lambda_b \rightarrow J/\psi p K$ process again [24]. Indeed, LHCb provided strong experimental evidence for the existence of the $\Sigma_c\bar{D}^{(*)}$ -type hidden-charm molecular pentaquarks [25–31]. In the following years, LHCb reported the evidence of the $P_{cs}(4459)$ [32] and observed the $P_{\psi s}^\Lambda(4338)$ [33]. These exciting experimental progresses not only make the hidden-charm pentaquark family becomes abundant [34–80], but also inspire theorists to explore the $P_{cs(s)}$ -type hidden-charm molecular pentaquarks [81–84]. In recent years, the study of the mass spectra of the hidden-charm molecular pentaquarks with double strangeness and triple strangeness has been carried out by the Lanzhou group, which are involved in the $\Xi_c^{(\prime,*)}\bar{D}_s^{(*)}$ [81] and $\Omega_c^{(*)}\bar{D}_s^{(*)}$ [82] interactions.

At present, the study of the properties of the hidden-charm

molecular pentaquarks is still an interesting and important research issue of hadron physics, which can provide useful clues for the construction of the family composed of the hidden-charm molecular pentaquarks. It is well known that the study of the electromagnetic properties is one of the effective approaches to reflect the inner structures of hadrons. A typical example is that the constituent quark model was successfully used to describe the magnetic moments of the decuplet and octet baryons successfully [85–87], where there were the corresponding experimental data [88]. Obviously, the electromagnetic properties of the hidden-charm molecular pentaquarks should be emphasised. So far, some discussions of the electromagnetic properties of the $\Sigma_c^{(*)}\bar{D}^{(*)}$ -type hidden-charm molecular pentaquarks and the $\Xi_c^{(\prime,*)}\bar{D}^{(*)}$ -type hidden-charm molecular pentaquarks with single strangeness have been given in the constituent quark model [89–92], which may reflect the inner structures of these discussed hidden-charm molecular pentaquarks. We should point out that these studies [89–92] of the electromagnetic properties of some hidden-charm molecular pentaquarks is still at the start stage. In this sense, we still need to continue our efforts to obtain the electromagnetic properties of other types of hidden-charm molecular pentaquarks.

In this paper, we focus on the $\Xi_c^{(\prime,*)}\bar{D}_s^*$ -type hidden-charm molecular pentaquarks with double strangeness and the $\Omega_c^{(*)}\bar{D}_s^*$ -type hidden-charm molecular pentaquarks with triple strangeness, which were predicted in Refs. [81, 82]. We study their electromagnetic properties including the magnetic moments, the transition magnetic moments, and the radiative decay behavior within the constituent quark model. In the realistic calculation, the S - D wave mixing effect and the coupled channel effect are taken into account. It is hoped that the present investigation will complete our knowledge of the hidden-charm molecular pentaquarks with double strangeness and triple strangeness [81, 82].

The remainder of this paper is organized as follows. In Sec. II, the calculation method of the electromagnetic properties of the hadronic molecules will be given. Meanwhile, the electromagnetic properties of the $\Xi_c^{(\prime,*)}\bar{D}_s^*$ molecular states will be presented. In Sec. III, the electromagnetic properties of the $\Omega_c^{(*)}\bar{D}_s^*$ molecular states are discussed. Finally, a short summary is given in Sec. IV.

* wangfl2016@lzu.edu.cn

† luosq15@lzu.edu.cn

‡ zhouhy20@lzu.edu.cn

§ liuzhanwei@lzu.edu.cn

¶ xiangliu@lzu.edu.cn

II. THE ELECTROMAGNETIC PROPERTIES OF THE $\Xi_c^{(*)}\bar{D}_s^*$ MOLECULAR STATES

In this section, we explore the electromagnetic properties including the magnetic moments, the transition magnetic moments, and the radiative decay behavior of the $\Xi_c'\bar{D}_s^*$ molecular state with $I(J^P) = 1/2(3/2^-)$ and the $\Xi_c^*\bar{D}_s^*$ molecular state with $I(J^P) = 1/2(5/2^-)$ [81], which may provide useful information to reflect their inner structures.

A. The magnetic moments and the transition magnetic moments of the $\Xi_c^{(*)}\bar{D}_s^*$ molecules

In the framework of the constituent quark model, the hadronic magnetic moment includes the spin magnetic moment and the orbital magnetic moment. In particular, the z -component of the spin magnetic moment operator of the hadron $\hat{\mu}_z^{\text{spin}}$ can be expressed as [85–87, 89–125]

$$\hat{\mu}_z^{\text{spin}} = \sum_i \frac{e_i}{2M_i} \hat{\sigma}_{iz}. \quad (1)$$

In the above expression, e_i , M_i , and $\hat{\sigma}_{iz}$ denote the charge, mass, and z -component of the Pauli spin operator of the i -th constituent of the hadron, respectively. For the hadronic molecule composed of the baryon and the meson, the z -component of the orbital magnetic moment operator $\hat{\mu}_z^{\text{orbital}}$ can be written as [89–94, 96, 98, 100, 104, 105, 108, 116]

$$\begin{aligned} \hat{\mu}_z^{\text{orbital}} &= \mu_{bm}^L \hat{L}_z \\ &= \left(\frac{M_b}{M_b + M_m} \frac{e_m}{2M_m} + \frac{M_m}{M_b + M_m} \frac{e_b}{2M_b} \right) \hat{L}_z, \end{aligned} \quad (2)$$

where the subscripts b and m denote the baryon and the meson, respectively, and \hat{L}_z denotes the z -component of the orbital angular momentum operator between the baryon and the meson.

As pointed out in Refs. [85–87, 89–125], the magnetic moments of the hadrons μ_H and the transition magnetic moments between the hadrons $\mu_{H \rightarrow H'}$ have often been estimated by calculating the expectation values of the z -component of the total magnetic moment operator $\hat{\mu}_z$ with $\hat{\mu}_z = \hat{\mu}_z^{\text{spin}} + \hat{\mu}_z^{\text{orbital}}$ in the previous theoretical work, which can be explicitly written as

$$\mu_H = \langle J_H, J_H | \hat{\mu}_z | J_H, J_H \rangle, \quad (3)$$

$$\mu_{H \rightarrow H'} = \langle J_{H'}, J_{H'} | \hat{\mu}_z | J_H, J_H \rangle^{J_z = \text{Min}\{J_H, J_{H'}\}}. \quad (4)$$

Here, $H^{(*)}$ stands for either the fundamental hadron or the compound hadron. In realistic calculations, the previous theoretical studies usually take the maximum value of the third component of the total angular momentum quantum number of the hadron to give the hadronic magnetic moment, and adopt the maximum third component of the total angular momentum quantum number of the lowest state of the total angular momentum to give the transition magnetic moment between the hadrons [85–87, 89–125]. In the present work, the adopted model and convention of calculating the hadronic magnetic moments and transition magnetic moments are the

same as the previous theoretical work [85–87, 89–125]. When calculating the matrix element $\langle \psi_{H^{(*)}} | \hat{\mu}_z | \psi_H \rangle$, we first need to discuss their wave functions, which include the color part, the flavor part, the spin part, and the spatial part. For the hadronic state, the color wave function is simply 1. Its flavor-spin wave function can be constructed on the basis of the symmetry constraint, while the spatial wave function can be obtained by studying the mass spectrum of the hadron quantitatively [92].

In the following, we study the magnetic moments and the transition magnetic moments of the $\Xi_c'\bar{D}_s^*$ molecule with $I(J^P) = 1/2(3/2^-)$ and the $\Xi_c^*\bar{D}_s^*$ molecular state with $I(J^P) = 1/2(5/2^-)$ by the following three cases:

- by only considering the S -wave component,
- by adding the contribution of the D -wave channels,
- under the coupled channel analysis.

By the above procedure, we may present the roles of the S - D wave mixing effect and the coupled channel effect on the electromagnetic properties of the $\Xi_c^{(*)}\bar{D}_s^*$ molecular states.

1. The case by only considering the S -wave component

First, we study the magnetic moments and the transition magnetic moments of the $\Xi_c'\bar{D}_s^*$ molecular state with $I(J^P) = 1/2(3/2^-)$ and the $\Xi_c^*\bar{D}_s^*$ molecule with $I(J^P) = 1/2(5/2^-)$ when only considering the S -wave component. Their flavor wave functions $|I, I_3\rangle$ can be written as [81]

$$\begin{aligned} \left| \frac{1}{2}, \frac{1}{2} \right\rangle &= |\Xi_c^{(*)+} D_s^{*-}\rangle, \\ \left| \frac{1}{2}, -\frac{1}{2} \right\rangle &= |\Xi_c^{(*)0} D_s^{*-}\rangle, \end{aligned}$$

where I and I_3 represent the isospins and isospin third components of the $\Xi_c^{(*)}\bar{D}_s^*$ systems, respectively. Meanwhile, their spin wave functions $|S, S_3\rangle$ can be constructed by the following coupling [81]

$$\begin{aligned} \Xi_c'\bar{D}_s^* : |S, S_3\rangle &= \sum_{S_{\Xi_c'}, S_{\bar{D}_s^*}} C_{\frac{1}{2} S_{\Xi_c'}, 1 S_{\bar{D}_s^*}}^{S S_3} \left| \frac{1}{2}, S_{\Xi_c'} \right\rangle |1, S_{\bar{D}_s^*}\rangle, \\ \Xi_c^*\bar{D}_s^* : |S, S_3\rangle &= \sum_{S_{\Xi_c^*}, S_{\bar{D}_s^*}} C_{\frac{3}{2} S_{\Xi_c^*}, 1 S_{\bar{D}_s^*}}^{S S_3} \left| \frac{3}{2}, S_{\Xi_c^*} \right\rangle |1, S_{\bar{D}_s^*}\rangle. \end{aligned}$$

In the above expressions, S and S_3 represent the spins and the third component of the spins of the $\Xi_c^{(*)}\bar{D}_s^*$ systems, respectively. In addition, $C_{ab,cd}^{ef}$ is the Clebsch-Gordan coefficient, while $S_{\Xi_c'}$, $S_{\Xi_c^*}$, and $S_{\bar{D}_s^*}$ denote the spin third components of the Ξ_c' , Ξ_c^* , and \bar{D}_s^* , respectively.

With the above preparations, we can obtain the magnetic moments of the $\Xi_c'\bar{D}_s^*$ molecule with $I(J^P) = 1/2(3/2^-)$ and the $\Xi_c^*\bar{D}_s^*$ molecular state with $I(J^P) = 1/2(5/2^-)$. For example,

$$\begin{aligned} \mu_{\Xi_c'\bar{D}_s^*|3/2^-}^{I_3=1/2} &= \left\langle \chi_{\Xi_c'^+ D_s^{*-}}^{\left|\frac{1}{2}, \frac{1}{2}\right\rangle, 1, 1} \right| \hat{\mu}_z \left| \chi_{\Xi_c'^+ D_s^{*-}}^{\left|\frac{1}{2}, \frac{1}{2}\right\rangle, 1, 1} \right\rangle \\ &= \mu_{\Xi_c'^+} + \mu_{D_s^{*-}}. \end{aligned} \quad (5)$$

Here, χ_f^s is the spin and flavor wave function of the discussed hadron, while the superscript s and subscript f stand for the spin wave function and the flavor wave function, respectively. In addition, when studying the hadronic magnetic moment with the single channel analysis, the overlap of its spatial wave function is 1, which is omitted in the above expression.

As for the magnetic moments of the $\Xi_c^{(*)}$ baryons and the \bar{D}_s^* meson, we calculate them within the constituent quark model. We first introduce the flavor and spin wave functions of the $\Xi_c^{(*)}$ baryons and the \bar{D}_s^* meson. Their flavor wave functions can be written as

$$\begin{aligned}\Xi_c^{(*)+} &: \frac{1}{\sqrt{2}}(usc + suc), \\ \Xi_c^{(*)0} &: \frac{1}{\sqrt{2}}(dsc + sdc), \\ D_s^{*-} &: \bar{c}s,\end{aligned}$$

while their corresponding spin wave functions $|S, S_3\rangle$ can be expressed as

$$\begin{aligned}\Xi_c' &: \begin{cases} \left| \frac{1}{2}, \frac{1}{2} \right\rangle = \frac{1}{\sqrt{6}}(2\uparrow\uparrow\downarrow - \downarrow\uparrow\uparrow - \uparrow\downarrow\uparrow) \\ \left| \frac{1}{2}, -\frac{1}{2} \right\rangle = \frac{1}{\sqrt{6}}(\downarrow\uparrow\downarrow + \uparrow\downarrow\downarrow - 2\downarrow\downarrow\uparrow) \end{cases}, \\ \Xi_c^* &: \begin{cases} \left| \frac{3}{2}, \frac{3}{2} \right\rangle = \uparrow\uparrow\uparrow \\ \left| \frac{3}{2}, \frac{1}{2} \right\rangle = \frac{1}{\sqrt{3}}(\downarrow\uparrow\uparrow + \uparrow\downarrow\uparrow + \uparrow\uparrow\downarrow) \\ \left| \frac{3}{2}, -\frac{1}{2} \right\rangle = \frac{1}{\sqrt{3}}(\downarrow\downarrow\uparrow + \uparrow\downarrow\downarrow + \downarrow\uparrow\downarrow) \\ \left| \frac{3}{2}, -\frac{3}{2} \right\rangle = \downarrow\downarrow\downarrow \end{cases}, \\ \bar{D}_s^* &: \begin{cases} |1, 1\rangle = \uparrow\uparrow \\ |1, 0\rangle = \frac{1}{\sqrt{2}}(\uparrow\downarrow + \downarrow\uparrow) \\ |1, -1\rangle = \downarrow\downarrow \end{cases}.\end{aligned}$$

Here, \uparrow and \downarrow represent the third components of the quark spin with $1/2$ and $-1/2$, respectively.

From the flavor and spin wave functions of the $\Xi_c^{(*)}$ baryons and the \bar{D}_s^* meson, we can calculate their magnetic moments. As an example, we deduce the magnetic moment of the Ξ_c^{*+} baryon as follows

$$\begin{aligned}\mu_{\Xi_c^{*+}} &= \left\langle \chi_{\frac{1}{\sqrt{2}}(usc+suc)}^{\frac{1}{\sqrt{6}}(2\uparrow\uparrow\downarrow-\downarrow\uparrow\uparrow-\uparrow\downarrow\uparrow)} \left| \hat{\mu}_z \right| \chi_{\frac{1}{\sqrt{2}}(usc+suc)}^{\frac{1}{\sqrt{6}}(2\uparrow\uparrow\downarrow-\downarrow\uparrow\uparrow-\uparrow\downarrow\uparrow)} \right\rangle \\ &= \frac{2}{3}\mu_u + \frac{2}{3}\mu_s - \frac{1}{3}\mu_c.\end{aligned}\quad (6)$$

In the present work, we define $\mu_q = -\mu_{\bar{q}} = e_q/2M_q$, where e_q stands for the quark charge and M_q is the constituent quark mass. In this way we can obtain the expressions for the magnetic moments of the $\Xi_c^{(*)}$ baryons and the \bar{D}_s^* meson. In the numerical analysis, we take the constituent quark masses as input, i.e., $M_u = 0.336$ GeV, $M_d = 0.336$ GeV,

$M_s = 0.450$ GeV, and $M_c = 1.680$ GeV, to study the electromagnetic properties of these discussed hadrons quantitatively, which are taken from Ref. [86] and widely used to discuss the magnetic moments of the hadronic molecular states [90, 92, 98].

In Table I, we collect the expressions and numerical results of the magnetic moments of the $\Xi_c^{(*)}$ baryons and the \bar{D}_s^* meson, where the present numerical results are in agreement with those in Refs. [86, 104, 107, 117, 126–129]. In this paper, the hadronic magnetic moments and transition magnetic moments are presented in the units of the nuclear magneton $\mu_N = e/2M_N$ with $M_N = 0.938$ GeV [88]. As shown in Table I, the Ξ_c^{*+} and Ξ_c^{*0} have different magnetic moments, while the magnetic moment of the Ξ_c^{*+} is different from that of the Ξ_c^{*0} , which is due to the magnetic magnetons of the up quark and down quark existing an obvious difference, i.e., $\mu_u = 1.862 \mu_N$ and $\mu_d = -0.931 \mu_N$. There are also approximately equal magnetic moments for the Ξ_c^{*0} and Ξ_c^{*0} .

TABLE I. The magnetic moments and the transition magnetic moments of the $\Xi_c^{(*)}$ baryons and the \bar{D}_s^* meson. Here, the magnetic moment and the transition magnetic moment are in units of μ_N , while the square brackets represent the expressions of their magnetic moments and transition magnetic moments in the second column.

Quantities	Our results	Other results
$\mu_{\Xi_c^{*+}}$	$0.654 \left[\frac{2}{3}\mu_u + \frac{2}{3}\mu_s - \frac{1}{3}\mu_c \right]$	0.65 [126], 0.67 [127]
$\mu_{\Xi_c^{*0}}$	$-1.208 \left[\frac{2}{3}\mu_d + \frac{2}{3}\mu_s - \frac{1}{3}\mu_c \right]$	-1.20 [128], -1.20 [127]
$\mu_{\Xi_c^{*+}}$	$1.539 [\mu_u + \mu_s + \mu_c]$	1.51 [129], 1.59 [104]
$\mu_{\Xi_c^{*0}}$	$-1.254 [\mu_d + \mu_s + \mu_c]$	-1.20 [117], -1.18 [107]
$\mu_{D_s^{*-}}$	$-1.067 [\mu_{\bar{c}} + \mu_s]$	-1.00 [117], -1.08 [127]
$\mu_{\Xi_c^{*+} \rightarrow \Xi_c^{*+}}$	$0.199 \left[\frac{\sqrt{2}}{3}(\mu_u + \mu_s - 2\mu_c) \right]$	0.17 [86], 0.16 [130]
$\mu_{\Xi_c^{*0} \rightarrow \Xi_c^{*0}}$	$-1.117 \left[\frac{\sqrt{2}}{3}(\mu_d + \mu_s - 2\mu_c) \right]$	-1.07 [117], -1.03 [117]

Based on the obtained magnetic moments of the $\Xi_c^{(*)}$ baryons and the \bar{D}_s^* meson, we can obtain the numerical results of the magnetic moments of the $\Xi_c' \bar{D}_s^*$ molecule with $I(J^P) = 1/2(3/2^-)$ and the $\Xi_c^* \bar{D}_s^*$ molecular state with $I(J^P) = 1/2(5/2^-)$. In Table II, we present the expressions and numerical results of the magnetic moments of the $\Xi_c' \bar{D}_s^*$ molecular state with $I(J^P) = 1/2(3/2^-)$ and the $\Xi_c^* \bar{D}_s^*$ molecular state with $I(J^P) = 1/2(5/2^-)$ when performing the single channel analysis.

As indicated in Table II, the magnetic moments of the $\Xi_c' \bar{D}_s^*[3/2^-]$ molecule with $I_3 = 1/2$, the $\Xi_c' \bar{D}_s^*[3/2^-]$ molecule with $I_3 = -1/2$, the $\Xi_c^* \bar{D}_s^*[5/2^-]$ molecule with $I_3 = 1/2$, and the $\Xi_c^* \bar{D}_s^*[5/2^-]$ molecule with $I_3 = -1/2$ are $-0.414 \mu_N$, $-2.275 \mu_N$, $0.472 \mu_N$, and $-2.321 \mu_N$, respectively. Because the magnetic moment of the $\Xi_c' \bar{D}_s^*[3/2^-]$ molecule can be written as the sum of the magnetic moments of the Ξ_c' baryon and the \bar{D}_s^* meson, and the magnetic moment of the Ξ_c^{*+} is significantly different from that of the Ξ_c^{*0} . Thus, the magnetic moment of the $\Xi_c' \bar{D}_s^*[3/2^-]$ molecule with $I_3 = 1/2$ is ob-

TABLE II. The expressions and values of the magnetic moments of the $\Xi'_c \bar{D}_s^*$ molecular state with $I(J^P) = 1/2(3/2^-)$ and the $\Xi_c^* \bar{D}_s^*$ molecular state with $I(J^P) = 1/2(5/2^-)$ when only the S -wave component is considered.

Physical quantities	Expressions	Values
$\mu_{\Xi'_c \bar{D}_s^* 3/2^-}^{I_3=1/2}$	$\mu_{\Xi_c^{*+}} + \mu_{D_s^{*-}}$	$-0.414 \mu_N$
$\mu_{\Xi'_c \bar{D}_s^* 3/2^-}^{I_3=-1/2}$	$\mu_{\Xi_c^{*0}} + \mu_{D_s^{*-}}$	$-2.275 \mu_N$
$\mu_{\Xi_c^* \bar{D}_s^* 5/2^-}^{I_3=1/2}$	$\mu_{\Xi_c^{*+}} + \mu_{D_s^{*-}}$	$0.472 \mu_N$
$\mu_{\Xi_c^* \bar{D}_s^* 5/2^-}^{I_3=-1/2}$	$\mu_{\Xi_c^{*0}} + \mu_{D_s^{*-}}$	$-2.321 \mu_N$

viously different from that with $I_3 = -1/2$. Similar to the $\Xi'_c \bar{D}_s^* | 3/2^- \rangle$ molecular state, the $\Xi_c^* \bar{D}_s^* | 5/2^- \rangle$ molecular state with different I_3 quantum numbers have different magnetic moments. In addition, there are almost identical magnetic moments for the $\Xi'_c \bar{D}_s^* | 3/2^- \rangle$ molecule with $I_3 = -1/2$ and $\Xi_c^* \bar{D}_s^* | 5/2^- \rangle$ molecule with $I_3 = -1/2$, since the magnetic moment of the Ξ_c^{*0} is close to that of the Ξ_c^{*0} .

Apart from studying the magnetic moments of the $\Xi'_c \bar{D}_s^*$ molecular state with $I(J^P) = 1/2(3/2^-)$ and the $\Xi_c^* \bar{D}_s^*$ molecule with $I(J^P) = 1/2(5/2^-)$, the study of their transition magnetic moments also can give useful hints to reflect their inner structures. For example, the transition magnetic moment between the $\Xi'_c \bar{D}_s^*$ molecule with $I(J^P) = 1/2(3/2^-)$ and the $\Xi_c^* \bar{D}_s^*$ molecular state with $I(J^P) = 1/2(5/2^-)$ with $I_3 = 1/2$ can be given by

$$\begin{aligned} & \mu_{\Xi'_c \bar{D}_s^* | 5/2^- \rightarrow \Xi_c^* \bar{D}_s^* | 3/2^-}^{I_3=1/2} \\ &= \left\langle \chi_{\Xi_c^{*+} \bar{D}_s^{*-}} \left| \hat{\mu}_z \left| \chi_{\Xi_c^{*+} \bar{D}_s^{*-}} \sqrt{\frac{3}{5}} \left| \frac{3}{2}, \frac{3}{2} \right\rangle | 1, 0 \rangle + \sqrt{\frac{3}{5}} \left| \frac{3}{2}, \frac{1}{2} \right\rangle | 1, 1 \rangle \right. \right\rangle \\ &= \sqrt{\frac{3}{5}} \mu_{\Xi_c^{*+} \rightarrow \Xi_c^{*+}}. \end{aligned} \quad (7)$$

Thus, the transition magnetic moment of the $\Xi_c^* \bar{D}_s^* | 5/2^- \rangle \rightarrow \Xi'_c \bar{D}_s^* | 3/2^- \rangle \gamma$ process can be related to that of the $\Xi_c^* \rightarrow \Xi'_c \gamma$ process. In the following, we further estimate the transition magnetic moment of the $\Xi_c^{*+} \rightarrow \Xi_c^{*+} \gamma$ process, which can be derived from

$$\begin{aligned} \mu_{\Xi_c^{*+} \rightarrow \Xi_c^{*+}} &= \left\langle \chi_{\frac{1}{\sqrt{3}}(\downarrow\downarrow\uparrow + \uparrow\downarrow\downarrow + \downarrow\uparrow\downarrow)} \left| \hat{\mu}_z \left| \chi_{\frac{1}{\sqrt{6}}(2\uparrow\downarrow - \downarrow\uparrow\uparrow - \uparrow\downarrow\uparrow)} \right. \right\rangle \\ &= \frac{\sqrt{2}}{3} (\mu_u + \mu_s - 2\mu_c). \end{aligned} \quad (8)$$

In Table I, the expressions and numerical results of the transition magnetic moments of the $\Xi_c^{*+} \rightarrow \Xi_c^{*+} \gamma$ and $\Xi_c^{*0} \rightarrow \Xi_c^{*0} \gamma$ processes are collected, where these results are comparable with the theoretical predictions of Refs. [86, 117, 130].

According to the numerical results of the transition magnetic moments of the $\Xi_c^{*+} \rightarrow \Xi_c^{*+} \gamma$ and $\Xi_c^{*0} \rightarrow \Xi_c^{*0} \gamma$ processes, we can obtain the values of the transition magnetic moments between the $\Xi'_c \bar{D}_s^*$ molecule with $I(J^P) = 1/2(3/2^-)$ and the $\Xi_c^* \bar{D}_s^*$ molecular state with $I(J^P) = 1/2(5/2^-)$, i.e.,

$$\begin{aligned} \mu_{\Xi'_c \bar{D}_s^* | 5/2^- \rightarrow \Xi'_c \bar{D}_s^* | 3/2^-}^{I_3=1/2} &= 0.154 \mu_N, \\ \mu_{\Xi'_c \bar{D}_s^* | 5/2^- \rightarrow \Xi'_c \bar{D}_s^* | 3/2^-}^{I_3=-1/2} &= -0.866 \mu_N. \end{aligned}$$

Here, we have to note that the absolute value of the transition magnetic moment of the $\Xi_c^{*0} \rightarrow \Xi_c^{*0}$ process is much larger than that of the $\Xi_c^{*+} \rightarrow \Xi_c^{*+}$ process [117, 130]. Thus, the value of $|\mu_{\Xi'_c \bar{D}_s^* | 5/2^- \rightarrow \Xi'_c \bar{D}_s^* | 3/2^-}|$ with $I_3 = -1/2$ is much larger than that of $|\mu_{\Xi'_c \bar{D}_s^* | 5/2^- \rightarrow \Xi'_c \bar{D}_s^* | 3/2^-}|$ with $I_3 = 1/2$.

2. The case by adding the contribution of the D -wave channels

We further study the magnetic moments and the transition magnetic moments of the $\Xi'_c \bar{D}_s^*$ molecular state with $I(J^P) = 1/2(3/2^-)$ and the $\Xi_c^* \bar{D}_s^*$ molecule with $I(J^P) = 1/2(5/2^-)$ by adding the contribution of the D -wave channels. In our calculation, we consider the following S -wave and D -wave channels for the $\Xi'_c \bar{D}_s^*$ molecular state with $I(J^P) = 1/2(3/2^-)$ and the $\Xi_c^* \bar{D}_s^*$ molecular state with $I(J^P) = 1/2(5/2^-)$ [81], i.e.,

$$\begin{aligned} \Xi'_c \bar{D}_s^* | 3/2^- \rangle &: |^4S_{3/2}\rangle, |^2D_{3/2}\rangle, |^4D_{3/2}\rangle, \\ \Xi_c^* \bar{D}_s^* | 5/2^- \rangle &: |^6S_{5/2}\rangle, |^2D_{5/2}\rangle, |^4D_{5/2}\rangle, |^6D_{5/2}\rangle. \end{aligned}$$

Here, we use $|^{2S+1}L_J\rangle$ to represent the spin S , the orbital angular momentum L , and the total angular momentum J for the discussed molecular states.

Taking into account the contribution of the S - D wave mixing effect, the magnetic moment and the transition magnetic moment of the molecular state can be deduced by

$$\sum_{i,j} \mu_{\mathcal{A}_i \rightarrow \mathcal{A}_j} \langle R_{\mathcal{A}_j} | R_{\mathcal{A}_i} \rangle, \quad (9)$$

$$\sum_{i,j} \mu_{\mathcal{B}_i \rightarrow \mathcal{B}_j} \langle R_{\mathcal{B}_j} | R_{\mathcal{B}_i} \rangle, \quad (10)$$

respectively. Here, \mathcal{A} and \mathcal{B} represent two discussed molecular states, while R_i represents the spatial wave function of the corresponding i -th channel.

If we add the contribution of the D -wave channels to study the electromagnetic properties of the molecular states, we need to introduce the procedure of obtaining the magnetic moments and the transition magnetic moments of the D -wave channels. For these discussed molecular states, their spin-orbital wave functions $|^{2S+1}L_J\rangle$ can be constructed by the coupling of the spin wave function $|S, m_S\rangle$ and the orbital wave function Y_{L, m_L} , which can be explicitly written as

$$|^{2S+1}L_J\rangle = \sum_{m_S, m_L} C_{S m_S, L m_L}^{J M} |S, m_S\rangle Y_{L, m_L}.$$

As the result, the magnetic moment of the $\Xi'_c \bar{D}_s^* |^2D_{3/2}\rangle$ channel with $I_3 = 1/2$ is given by

$$\begin{aligned} \mu_{\Xi'_c \bar{D}_s^* |^2D_{3/2}\rangle}^{I_3=1/2} &= \frac{1}{5} \left(-\frac{1}{3} \mu_{\Xi_c^{*+}} + \frac{2}{3} \mu_{D_s^{*-}} + \mu_{\Xi_c^{*+} D_s^{*-}}^L \right) \\ &\quad + \frac{4}{5} \left(\frac{1}{3} \mu_{\Xi_c^{*+}} - \frac{2}{3} \mu_{D_s^{*-}} + 2\mu_{\Xi_c^{*+} D_s^{*-}}^L \right) \\ &= \frac{1}{5} \mu_{\Xi_c^{*+}} - \frac{2}{5} \mu_{D_s^{*-}} + \frac{9}{5} \mu_{\Xi_c^{*+} D_s^{*-}}^L, \end{aligned} \quad (11)$$

while the transition magnetic moment of the $\Xi_c' \bar{D}_s^* |^4 D_{3/2} \rangle \rightarrow \Xi_c' \bar{D}_s^* |^2 D_{3/2} \rangle$ process with $I_3 = 1/2$ can be derived as

$$\begin{aligned} \mu_{\Xi_c' \bar{D}_s^* |^4 D_{3/2} \rightarrow \Xi_c' \bar{D}_s^* |^2 D_{3/2}}^{I_3=1/2} &= -\frac{\sqrt{2}}{5} \left(\frac{2\sqrt{2}}{3} \mu_{\Xi_c'^+} - \frac{\sqrt{2}}{3} \mu_{D_s^{*-}} \right) \\ &\quad - \frac{2\sqrt{2}}{5} \left(\frac{2\sqrt{2}}{3} \mu_{\Xi_c'^+} - \frac{\sqrt{2}}{3} \mu_{D_s^{*-}} \right) \\ &= -\frac{4}{5} \mu_{\Xi_c'^+} + \frac{2}{5} \mu_{D_s^{*-}}. \end{aligned} \quad (12)$$

Using the above procedure, we can obtain the magnetic moments and the transition magnetic moments of the D -wave channels involved in our calculation.

From Eqs. (9)-(10), the magnetic moments and the transition magnetic moments of the hadronic molecules depend on the relevant mixing channel components $\langle R_{\mathcal{A}_j} | R_{\mathcal{A}_i} \rangle$ and $\langle R_{\mathcal{B}_j} | R_{\mathcal{A}_i} \rangle$ when performing the S - D wave mixing analysis, which are related to the binding energies for the discussed molecular states. Since these discussed molecules are still missing in experiment, we adopt three typical binding energies -0.5 MeV, -6.0 MeV, and -12.0 MeV for the $\Xi_c' \bar{D}_s^*$ molecular state with $I(J^P) = 1/2(3/2^-)$ and the $\Xi_c^* \bar{D}_s^*$ molecule with $I(J^P) = 1/2(5/2^-)$ to present their magnetic moments and transition magnetic moments, where the different binding energies mainly come from the different fine-tuning cutoff values in the mass spectrum analysis. The corresponding numerical results are given in Table IV.

TABLE III. The magnetic moments and the transition magnetic moments of the $\Xi_c' \bar{D}_s^*$ molecular state with $I(J^P) = 1/2(3/2^-)$ and the $\Xi_c^* \bar{D}_s^*$ molecular state with $I(J^P) = 1/2(5/2^-)$.

I_3	Physical quantities	Values
$\frac{1}{2}$	$\mu_{\Xi_c' \bar{D}_s^* ^3 3/2^-}$	$-0.414 \mu_N, -0.416 \mu_N, -0.416 \mu_N$
	$\mu_{\Xi_c^* \bar{D}_s^* ^5 5/2^-}$	$0.472 \mu_N, 0.472 \mu_N, 0.472 \mu_N$
	$\mu_{\Xi_c' \bar{D}_s^* ^5 5/2^- \rightarrow \Xi_c' \bar{D}_s^* ^3 3/2^-}$	$0.154 \mu_N, 0.154 \mu_N, 0.154 \mu_N$
$-\frac{1}{2}$	$\mu_{\Xi_c' \bar{D}_s^* ^3 3/2^-}$	$-2.272 \mu_N, -2.264 \mu_N, -2.261 \mu_N$
	$\mu_{\Xi_c^* \bar{D}_s^* ^5 5/2^-}$	$-2.320 \mu_N, -2.319 \mu_N, -2.319 \mu_N$
	$\mu_{\Xi_c' \bar{D}_s^* ^5 5/2^- \rightarrow \Xi_c' \bar{D}_s^* ^3 3/2^-}$	$-0.865 \mu_N, -0.864 \mu_N, -0.864 \mu_N$

For the obtained magnetic moments and transition magnetic moments of the $\Xi_c' \bar{D}_s^*$ molecule with $I(J^P) = 1/2(3/2^-)$ and the $\Xi_c^* \bar{D}_s^*$ molecular state with $I(J^P) = 1/2(5/2^-)$ after adding the contribution of the D -wave channels, we want to specify two points: (1) The S - D wave mixing effect is not obvious to the magnetic moments and the transition magnetic moments of the $\Xi_c' \bar{D}_s^*$ molecular state with $I(J^P) = 1/2(3/2^-)$ and the $\Xi_c^* \bar{D}_s^*$ molecule with $I(J^P) = 1/2(5/2^-)$. Here, the variations of their magnetic moments and transition magnetic moments are less than $0.014 \mu_N$ after considering the contribution of the S - D wave mixing effect, which is due to the S -wave channels have the dominant contributions with the probabilities over 99% and play the important role in forming the loosely bound

states for the $\Xi_c' \bar{D}_s^*$ state with $I(J^P) = 1/2(3/2^-)$ and the $\Xi_c^* \bar{D}_s^*$ state with $I(J^P) = 1/2(5/2^-)$ [81]; (2) Since the relevant mixing channel components are less dependent on the binding energies for the $\Xi_c' \bar{D}_s^*$ molecule with $I(J^P) = 1/2(3/2^-)$ and the $\Xi_c^* \bar{D}_s^*$ molecular state with $I(J^P) = 1/2(5/2^-)$ [81], their electromagnetic properties do not significantly depend on their binding energies.

3. The case under the coupled channel analysis

We continue to study the magnetic moments and the transition magnetic moments of these discussed molecular states in the coupled channel analysis. For the $\Xi_c' \bar{D}_s^*$ molecular state with $I(J^P) = 1/2(3/2^-)$, we can further consider the contribution of the coupled channel effect from the $\Xi_c' \bar{D}_s^*$ and $\Xi_c^* \bar{D}_s^*$ systems [81].

Considering the coupled channel effect with two channels \mathcal{A} and \mathcal{B} , the magnetic moment of the molecular state can be derived by

$$\begin{aligned} &\sum_{i,j} \mu_{\mathcal{A}_i \rightarrow \mathcal{A}_j} \langle R_{\mathcal{A}_j} | R_{\mathcal{A}_i} \rangle + \sum_{i,j} \mu_{\mathcal{B}_i \rightarrow \mathcal{B}_j} \langle R_{\mathcal{B}_j} | R_{\mathcal{B}_i} \rangle \\ &+ \sum_{i,j} \mu_{\mathcal{B}_i \rightarrow \mathcal{A}_j} \langle R_{\mathcal{A}_j} | R_{\mathcal{B}_i} \rangle + \sum_{i,j} \mu_{\mathcal{A}_i \rightarrow \mathcal{B}_j} \langle R_{\mathcal{B}_j} | R_{\mathcal{A}_i} \rangle, \end{aligned} \quad (13)$$

while the transition magnetic moment between the molecular states can be given by

$$\begin{aligned} &\sum_{i,j} \mu_{\mathcal{A}_i \rightarrow \mathcal{C}_j} \langle R_{\mathcal{C}_j} | R_{\mathcal{A}_i} \rangle + \sum_{i,j} \mu_{\mathcal{A}_i \rightarrow \mathcal{D}_j} \langle R_{\mathcal{D}_j} | R_{\mathcal{A}_i} \rangle \\ &+ \sum_{i,j} \mu_{\mathcal{B}_i \rightarrow \mathcal{C}_j} \langle R_{\mathcal{C}_j} | R_{\mathcal{B}_i} \rangle + \sum_{i,j} \mu_{\mathcal{B}_i \rightarrow \mathcal{D}_j} \langle R_{\mathcal{D}_j} | R_{\mathcal{B}_i} \rangle. \end{aligned} \quad (14)$$

By performing several lengthy and tedious deductions, we obtain the magnetic moments and the transition magnetic moments of these discussed hidden-charm molecular pentaquarks with double strangeness when performing the coupled channel analysis, and the relevant numerical results are presented in Table IV. Here, we take three typical binding energies -0.5 MeV, -6.0 MeV, and -12.0 MeV for the investigated molecular states when presenting these numerical results.

TABLE IV. The magnetic moments and the transition magnetic moments of these discussed hidden-charm molecular pentaquarks with double strangeness when performing the coupled channel analysis.

Physical quantities	Values
$\mu_{\Xi_c' \bar{D}_s^* ^3 3/2^-}^{I_3=1/2}$	$-0.389 \mu_N, -0.335 \mu_N, -0.308 \mu_N$
$\mu_{\Xi_c' \bar{D}_s^* ^3 3/2^-}^{I_3=-1/2}$	$-2.305 \mu_N, -2.354 \mu_N, -2.370 \mu_N$
$\mu_{\Xi_c^* \bar{D}_s^* ^5 5/2^- \rightarrow \Xi_c' \bar{D}_s^* ^3 3/2^-}^{I_3=1/2}$	$0.088 \mu_N, -0.039 \mu_N, -0.091 \mu_N$
$\mu_{\Xi_c^* \bar{D}_s^* ^5 5/2^- \rightarrow \Xi_c' \bar{D}_s^* ^3 3/2^-}^{I_3=-1/2}$	$-0.866 \mu_N, -0.864 \mu_N, -0.862 \mu_N$

After including the contribution of the coupled channel effect, the magnetic moments and the transition magnetic

moments of these discussed hidden-charm molecular pentaquarks with double strangeness can be modified, where the most obvious change happens to the transition magnetic moment of the $\Xi_c^* \bar{D}_s^* [5/2^-] \rightarrow \Xi_c' \bar{D}_s^* [3/2^-]$ process with $I_3 = 1/2$, which can reach up to $0.245 \mu_N$.

Since the $\Xi_c^* \bar{D}_s^*$ and $\Omega_c^* \bar{D}^*$ thresholds are close to each other, the $\Omega_c^* \bar{D}^*$ channel may affect the magnetic moments of the $\Xi_c^* \bar{D}_s^*$ molecule with $I(J^P) = 1/2(5/2^-)$. In the following, we discuss the magnetic moments of the $\Xi_c^* \bar{D}_s^*$ molecule with $I(J^P) = 1/2(5/2^-)$ after considering the mixing of the $\Xi_c^* \bar{D}_s^*$ and $\Omega_c^* \bar{D}^*$ channels. As the important input information, we need to study the mass spectrum of the $\Xi_c^* \bar{D}_s^* / \Omega_c^* \bar{D}^*$ coupled channel system. To obtain the effective potentials in the coordinate space for the $\Xi_c^* \bar{D}_s^* / \Omega_c^* \bar{D}^*$ coupled channel system, we adopt the one-boson-exchange model in our calculation [9]. First, we can write out the concrete scattering amplitudes $\mathcal{M}^{h_1 h_2 \rightarrow h_3 h_4}$ for the $h_1 h_2 \rightarrow h_3 h_4$ processes according to the effective Lagrangian approach, and the relevant effective Lagrangians for the description of the heavy hadrons $\bar{D}^* / \mathcal{B}_6^*$ coupling with the light mesons are constructed as [131–138]

$$\mathcal{L}_{\bar{D}^* \bar{D}^* \sigma} = 2g_S \bar{D}_{a\mu}^* \bar{D}_a^{*\mu} \sigma, \quad (15)$$

$$\mathcal{L}_{\bar{D}^* \bar{D}^* \mathbb{P}} = \frac{2ig}{f_\pi} v^\alpha \varepsilon_{\alpha\mu\nu\lambda} \bar{D}_a^{*\mu} \bar{D}_b^{*\lambda} \partial^\nu \mathbb{P}_{ab}, \quad (16)$$

$$\mathcal{L}_{\bar{D}^* \bar{D}^* \mathbb{V}} = -\sqrt{2}\beta g_V \bar{D}_{a\mu}^* \bar{D}_b^{*\mu} v \cdot \mathbb{V}_{ab} - 2\sqrt{2}i\lambda g_V \bar{D}_a^{*\mu} \bar{D}_b^{*\nu} (\partial_\mu \mathbb{V}_\nu - \partial_\nu \mathbb{V}_\mu)_{ab}, \quad (17)$$

$$\mathcal{L}_{\mathcal{B}_6^* \mathcal{B}_6^* \sigma} = l_S \langle \bar{\mathcal{B}}_{6\mu}^* \sigma \mathcal{B}_6^{*\mu} \rangle, \quad (18)$$

$$\mathcal{L}_{\mathcal{B}_6^* \mathcal{B}_6^* \mathbb{P}} = -i \frac{3g_1}{2f_\pi} \varepsilon^{\mu\nu\lambda\kappa} v_\kappa \langle \bar{\mathcal{B}}_{6\mu}^* \partial_\nu \mathbb{P} \mathcal{B}_{6\lambda}^* \rangle, \quad (19)$$

$$\mathcal{L}_{\mathcal{B}_6^* \mathcal{B}_6^* \mathbb{V}} = \frac{\beta_S g_V}{\sqrt{2}} \langle \bar{\mathcal{B}}_{6\mu}^* v \cdot \mathbb{V} \mathcal{B}_6^{*\mu} \rangle + i \frac{\lambda_S g_V}{\sqrt{2}} \langle \bar{\mathcal{B}}_{6\mu}^* (\partial^\mu \mathbb{V}^\nu - \partial^\nu \mathbb{V}^\mu) \mathcal{B}_{6\nu}^* \rangle. \quad (20)$$

Here, $v = (1, \mathbf{0})$ is the four velocity, and the matrices \mathcal{B}_6^* , \mathbb{P} , and \mathbb{V}_μ can be written as

$$\mathcal{B}_6^* = \begin{pmatrix} \Sigma_c^{*++} & \frac{\Sigma_c^{*+}}{\sqrt{2}} & \frac{\Xi_c^{*++}}{\sqrt{2}} \\ \frac{\Sigma_c^{*+}}{\sqrt{2}} & \Sigma_c^{*0} & \frac{\Xi_c^{*+0}}{\sqrt{2}} \\ \frac{\Xi_c^{*++}}{\sqrt{2}} & \frac{\Xi_c^{*+0}}{\sqrt{2}} & \Omega_c^{*0} \end{pmatrix}, \quad (21)$$

$$\mathbb{P} = \begin{pmatrix} \frac{\pi^0}{\sqrt{2}} + \frac{\eta}{\sqrt{6}} & \pi^+ & K^+ \\ \pi^- & -\frac{\pi^0}{\sqrt{2}} + \frac{\eta}{\sqrt{6}} & K^0 \\ K^- & \bar{K}^0 & -\sqrt{\frac{2}{3}}\eta \end{pmatrix},$$

$$\mathbb{V}_\mu = \begin{pmatrix} \frac{\rho^0}{\sqrt{2}} + \frac{\omega}{\sqrt{2}} & \rho^+ & K^{*+} \\ \rho^- & -\frac{\rho^0}{\sqrt{2}} + \frac{\omega}{\sqrt{2}} & K^{*0} \\ K^{*-} & \bar{K}^{*0} & \phi \end{pmatrix}_\mu,$$

respectively. In the effective Lagrangians above, the values of these coupling constants are $l_S = 6.20$, $g_S = 0.76$, $g_1 = 0.94$, $g = 0.59$, $f_\pi = 132$ MeV, $\beta_S g_V = 10.14$, $\beta g_V = -5.25$, $\lambda_S g_V = 19.2$ GeV⁻¹, and $\lambda g_V = -3.27$ GeV⁻¹

[139]. And then, the effective potentials in the momentum space can be related to the scattering amplitudes in terms of the Breit approximation, which can be written as $\mathcal{V}_E^{h_1 h_2 \rightarrow h_3 h_4}(\mathbf{q}) = -\mathcal{M}^{h_1 h_2 \rightarrow h_3 h_4} / \sqrt{2m_{h_1} 2m_{h_2} 2m_{h_3} 2m_{h_4}}$. Finally, the effective potentials in the coordinate space can be obtained by performing the Fourier transform, i.e., $\mathcal{V}_E^{h_1 h_2 \rightarrow h_3 h_4}(\mathbf{r}) = \int \frac{d^3 q}{(2\pi)^3} e^{i\mathbf{q} \cdot \mathbf{r}} \mathcal{V}_E^{h_1 h_2 \rightarrow h_3 h_4}(\mathbf{q}) \mathcal{F}^2(q^2, m_E^2)$. Here, we introduce the monopole type form factor $\mathcal{F}(q^2, m_E^2) = (\Lambda^2 - m_E^2) / (\Lambda^2 - q^2)$ in each interaction vertex, which is due to the fact that the discussed hadrons are not point-like particles. With the above preparation, we can deduce the effective potentials in the coordinate space for the $\Xi_c^* \bar{D}_s^* / \Omega_c^* \bar{D}^*$ coupled channel system, which include

$$\mathcal{V}_{\Xi_c^* \bar{D}_s^* \rightarrow \Xi_c^* \bar{D}_s^*} = -l_S g_S \mathcal{A}_1 Y_\sigma - \frac{81g}{12f_\pi^2} [\mathcal{A}_2 \mathcal{O}_r + \mathcal{A}_3 \mathcal{P}_r] Y_\eta - \frac{\beta \beta_S g_V^2}{4} \mathcal{A}_1 Y_\phi + \frac{\lambda \lambda_S g_V^2}{6} [2\mathcal{A}_2 \mathcal{O}_r - \mathcal{A}_3 \mathcal{P}_r] Y_\phi, \quad (22)$$

$$\mathcal{V}_{\Xi_c^* \bar{D}_s^* \rightarrow \Omega_c^* \bar{D}^*} = -\frac{81g}{2\sqrt{2}f_\pi^2} [\mathcal{A}_2 \mathcal{O}_r + \mathcal{A}_3 \mathcal{P}_r] Y_{K0} - \frac{\beta \beta_S g_V^2}{2\sqrt{2}} \mathcal{A}_1 Y_{K^*0} + \frac{\lambda \lambda_S g_V^2}{3\sqrt{2}} [2\mathcal{A}_2 \mathcal{O}_r - \mathcal{A}_3 \mathcal{P}_r] Y_{K^*0}, \quad (23)$$

$$\mathcal{V}_{\Omega_c^* \bar{D}^* \rightarrow \Omega_c^* \bar{D}^*} = \frac{81g}{6f_\pi^2} [\mathcal{A}_2 \mathcal{O}_r + \mathcal{A}_3 \mathcal{P}_r] Y_\eta, \quad (24)$$

where $\mathcal{O}_r = \frac{1}{r^2} \frac{\partial}{\partial r} r^2 \frac{\partial}{\partial r}$, $\mathcal{P}_r = r \frac{\partial}{\partial r} \frac{1}{r} \frac{\partial}{\partial r}$, and the function Y_i is defined as

$$Y_i = \frac{e^{-m_i r} - e^{-\Lambda_i r}}{4\pi r} - \frac{\Lambda_i^2 - m_i^2}{8\pi \Lambda_i} e^{-\Lambda_i r}. \quad (25)$$

Here, $m_i = \sqrt{m^2 - q_i^2}$ and $\Lambda_i = \sqrt{\Lambda^2 - q_i^2}$ with $q_0 = 0.113$ GeV. In the above effective potentials, we also introduce three operators, i.e.,

$$\mathcal{A}_1 = \sum_{a,b,m,n} C_{\frac{1}{2}a,1b}^{\frac{3}{2},a+b} C_{\frac{1}{2}m,1n}^{\frac{3}{2},m+n} \chi_3^{\dagger a} (\epsilon_1^n \cdot \epsilon_3^{\dagger b}) (\epsilon_2 \cdot \epsilon_4^{\dagger}) \chi_1^m,$$

$$\mathcal{A}_2 = \sum_{a,b,m,n} C_{\frac{1}{2}a,1b}^{\frac{3}{2},a+b} C_{\frac{1}{2}m,1n}^{\frac{3}{2},m+n} \chi_3^{\dagger a} (\epsilon_1^n \times \epsilon_3^{\dagger b}) \cdot (\epsilon_2 \times \epsilon_4^{\dagger}) \chi_1^m,$$

$$\mathcal{A}_3 = \sum_{a,b,m,n} C_{\frac{1}{2}a,1b}^{\frac{3}{2},a+b} C_{\frac{1}{2}m,1n}^{\frac{3}{2},m+n} \chi_3^{\dagger a} S(\epsilon_1^n \times \epsilon_3^{\dagger b}, \epsilon_2 \times \epsilon_4^{\dagger}, \hat{r}) \chi_1^m.$$

Here, we define $S(\mathbf{x}, \mathbf{y}, \hat{r}) = 3(\hat{r} \cdot \mathbf{x})(\hat{r} \cdot \mathbf{y}) - \mathbf{x} \cdot \mathbf{y}$. These operators should be sandwiched by the spin-orbital wave functions of the initial state and the final state, and the corresponding operator matrix elements with $J = 5/2$ are $\mathcal{A}_1 = \text{diag}(1, 1, 1, 1)$, $\mathcal{A}_2 = \text{diag}(-1, \frac{5}{3}, \frac{2}{3}, -1)$, and $\mathcal{A}_3 =$

$$\begin{pmatrix} 0 & \frac{2}{\sqrt{15}} & \frac{\sqrt{7}}{5\sqrt{3}} & -\frac{2\sqrt{14}}{5} \\ \frac{2}{\sqrt{15}} & 0 & \frac{\sqrt{7}}{3\sqrt{5}} & -\frac{4\sqrt{2}}{\sqrt{105}} \\ \frac{\sqrt{7}}{5\sqrt{3}} & \frac{\sqrt{7}}{3\sqrt{5}} & -\frac{16}{21} & -\frac{\sqrt{2}}{7\sqrt{3}} \\ -\frac{2\sqrt{14}}{5} & -\frac{4\sqrt{2}}{\sqrt{105}} & -\frac{\sqrt{2}}{7\sqrt{3}} & -\frac{4}{7} \end{pmatrix}. \quad \text{Based on the obtained ef-}$$

fective potentials in the coordinate space for the $\Xi_c^* \bar{D}_s^* / \Omega_c^* \bar{D}^*$ coupled channel system, we can obtain the bound state solutions for the $\Xi_c^* \bar{D}_s^* / \Omega_c^* \bar{D}^*$ coupled channel system with $I(J^P) = 1/2(5/2^-)$ by solving the coupled channel Schrödinger equation. In Table V, the relevant results are collected, and the calculation also gives the probabilities of these involved channels, which is the important input information when discussing the magnetic moments of the $\Xi_c^* \bar{D}_s^* / \Omega_c^* \bar{D}^*$ coupled channel system with $I(J^P) = 1/2(5/2^-)$.

TABLE V. Bound state solutions for the $\Xi_c^* \bar{D}_s^* / \Omega_c^* \bar{D}^*$ coupled channel system with $I(J^P) = 1/2(5/2^-)$.

Λ (GeV)	E (MeV)	r_{RMS} (fm)	$P(\Xi_c^* \bar{D}_s^* / \Omega_c^* \bar{D}^*)$
1.544	-0.536	3.746	97.129 /2.871
1.575	-6.086	1.154	88.923 /11.077
1.593	-12.188	0.813	84.560 /15.440

Furthermore, one gets $\mu_{\Omega_c^{*0}} = -1.018 \mu_N$, $\mu_{\bar{D}^{*0}} = 1.489 \mu_N$, and $\mu_{D^{*-}} = -1.303 \mu_N$ within the constituent quark model. In Table VI, we compare the obtained magnetic moments with and without considering the $\Omega_c^* \bar{D}^*$ channel. From Table VI, we can see the $\Omega_c^* \bar{D}^*$ channel hardly affects the magnetic moments of the $\Xi_c^* \bar{D}_s^*$ molecule with $I(J^P) = 1/2(5/2^-)$, which is due to the $\Xi_c^* \bar{D}_s^*$ as the dominant channel with the probability over 80%. In fact, the mainly reason is that the magnetic moment of the $\Xi_c^* \bar{D}_s^*$ state with $I(J^P) = 1/2(5/2^-)$ is extremely close to that of the $\Omega_c^* \bar{D}^*$ state with $I(J^P) = 1/2(5/2^-)$, which shows the results in the same row no difference with four effective numbers.

TABLE VI. The magnetic moments of the pure $\Xi_c^* \bar{D}_s^*$ and the mixing $\Xi_c^* \bar{D}_s^* / \Omega_c^* \bar{D}^*$ molecular states with $I(J^P) = 1/2(5/2^-)$.

$I_3(J^P)$	$\mu_{\Xi_c^* \bar{D}_s^*}$	$\mu_{\Xi_c^* \bar{D}_s^* / \Omega_c^* \bar{D}^*}$
$1/2(5/2^-)$	$0.472 \mu_N$	$0.472 \mu_N$
$-1/2(5/2^-)$	$-2.321 \mu_N$	$-2.321 \mu_N$

B. The radiative decay behavior of the $\Xi_c^{(*)} \bar{D}_s^*$ molecules

Experimentally, the radiative decay process is the ideal platform to study the hadronic electromagnetic properties. In the following, we simply estimate the radiative decay behavior between the $\Xi_c^* \bar{D}_s^*$ molecular state with $I(J^P) = 1/2(3/2^-)$ and the $\Xi_c^* \bar{D}_s^*$ molecule with $I(J^P) = 1/2(5/2^-)$ after obtaining their transition magnetic moments. For the radiative decay process $H \rightarrow H' \gamma$, the decay width $\Gamma_{H \rightarrow H' \gamma}$ can be related to the corresponding transition magnetic moment [90, 92, 98, 103, 109, 111, 115, 117–122, 125, 140], and the

general relation can be written as

$$\Gamma_{H \rightarrow H' \gamma} = \alpha_{\text{EM}} \frac{E_\gamma^3}{M_P^2} \frac{1}{2J_H + 1} \sum_{J_{H'z}} \left(\frac{\langle J_{H'}, J_{H'z} | \hat{\mu}_z | J_H, J_{Hz} \rangle}{\mu_N} \right)^2, \quad (26)$$

where α_{EM} is the electromagnetic fine structure constant with $\alpha_{\text{EM}} \approx 1/137$, the proton mass M_P is taken to be 0.938 GeV [88], and E_γ is the photon momentum, which is defined by

$$E_\gamma = \frac{M_H^2 - M_{H'}^2}{2M_H}.$$

The derivation of the formula for the radiative decay width related to the transition magnetic moment is given in Appendix A. In this paper, the masses of the S -wave charmed baryons and the S -wave charmed-strange meson are taken from the Particle Data Group [88].

In fact, the spatial wave functions of the initial and final states were not included in the above formula for the radiative decay width related to the transition magnetic moment. If the momentum of the emitted photon is particularly small, the spatial wave function of the emitted photon $e^{-ik \cdot r_i}$ is approximately equal to 1. Furthermore, the overlap of the spatial wave functions of the initial and final molecular states is approximately equal to 1 when their binding energies are similar. Thus, the spatial wave functions of the initial and final states do not affect the final result of the radiative decay width if the momentum of the emitted photon is particularly small and the binding energies of the initial and final molecules are similar. This approximation has been used to study the radiative decay width of the transition between the baryons or the transition between the mesons as shown in Refs. [103, 109, 111, 115, 117–122, 125]. However, the momentum of the emitted photon is about 60 MeV for the $\Xi_c^* \bar{D}_s^* |5/2^- \rangle \rightarrow \Xi_c' \bar{D}_s^* |3/2^- \rangle \gamma$ process, and we should consider the contribution of the spatial wave function of the emitted photon to the radiative decay width of the $\Xi_c^* \bar{D}_s^* |5/2^- \rangle \rightarrow \Xi_c' \bar{D}_s^* |3/2^- \rangle \gamma$ process. In the following, we will introduce how to take into account the contribution of the spatial wave functions of the initial and final states to the radiative decay width.

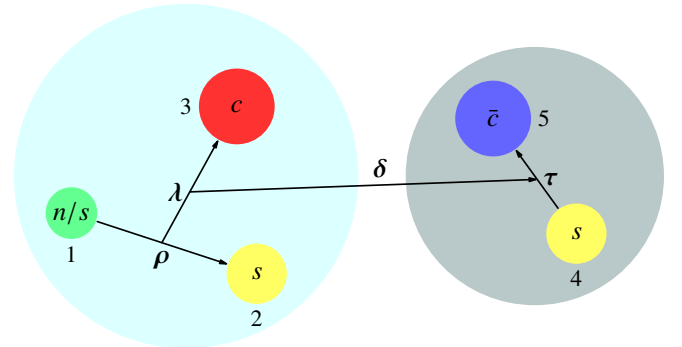


FIG. 1. The Jacobi coordinates of the $\Xi_c^{(*)} \bar{D}_s^* / \Omega_c^{(*)} \bar{D}_s^*$ -type hadronic molecular states.

To estimate the contribution of the spatial wave functions of the initial and final states to the radiative decay width, we need

to consider the spatial wave functions of the emitted photon $e^{-i\mathbf{k}\cdot\mathbf{r}_i}$ ($i = 1 - 5$) in the standard helicity transition amplitude $\mathcal{A}_{J_{fz}}^M$ for the magnetic operators [141], i.e.,

$$\mathcal{A}_{J_{fz}}^M = i\sqrt{\frac{E_\gamma}{2}}\langle\psi_f|\sum_j\frac{e_j}{2M_j}\hat{\sigma}_j\cdot(\boldsymbol{\epsilon}\times\hat{\mathbf{k}})e^{-i\mathbf{k}\cdot\mathbf{r}_j}|\psi_i\rangle. \quad (27)$$

Therefore, the main task is to deduce the matrix element $\langle\psi_f|\sum_j\hat{\sigma}_j e^{-i\mathbf{k}\cdot\mathbf{r}_j}|\psi_i\rangle$. As shown in Fig. 1, the Jacobi coordinates $\mathbf{R} = \{\boldsymbol{\rho}, \boldsymbol{\lambda}, \boldsymbol{\tau}, \boldsymbol{\delta}\}$ are used to represent the spatial wave functions of the hadronic molecular states, which are defined as

$$\begin{aligned} \boldsymbol{\rho} &= \mathbf{r}_2 - \mathbf{r}_1, \\ \boldsymbol{\lambda} &= \mathbf{r}_3 - \frac{m_1\mathbf{r}_1 + m_2\mathbf{r}_2}{m_1 + m_2}, \\ \boldsymbol{\tau} &= \mathbf{r}_5 - \mathbf{r}_4, \\ \boldsymbol{\delta} &= \frac{m_4\mathbf{r}_4 + m_5\mathbf{r}_5}{m_4 + m_5} - \frac{m_1\mathbf{r}_1 + m_2\mathbf{r}_2 + m_3\mathbf{r}_3}{m_1 + m_2 + m_3}. \end{aligned} \quad (28)$$

Thus, the spatial wave functions of the initial and final states can be explicitly expressed as $\psi(\boldsymbol{\rho})\psi(\boldsymbol{\lambda})\psi(\boldsymbol{\tau})\psi(\boldsymbol{\delta})$. On the other hand, the coordinates of the quarks \mathbf{r}_i ($i = 1 - 5$) can be written as

$$\mathbf{r}_i = \sum_j \alpha_{ij}\mathbf{R}_j = \alpha_{i1}\boldsymbol{\rho} + \alpha_{i2}\boldsymbol{\lambda} + \alpha_{i3}\boldsymbol{\tau} + \alpha_{i4}\boldsymbol{\delta}. \quad (29)$$

Thus, the \mathbf{r}_i can be represented by the linear combinations of the Jacobi coordinates, and the $\mathbf{k}\cdot\mathbf{r}_i$ can be expanded by

$$\mathbf{k}\cdot\mathbf{r}_i = \alpha_{i1}\mathbf{k}\cdot\boldsymbol{\rho} + \alpha_{i2}\mathbf{k}\cdot\boldsymbol{\lambda} + \alpha_{i3}\mathbf{k}\cdot\boldsymbol{\tau} + \alpha_{i4}\mathbf{k}\cdot\boldsymbol{\delta}. \quad (30)$$

For convenience, we use the matrix form to present the values of the matrix α , which is

$$\alpha = \begin{pmatrix} -\frac{m_2}{m_1+m_2} & -\frac{m_3}{m_1+m_2+m_3} & 0 & -\frac{m_4+m_5}{m_1+m_2+m_3+m_4+m_5} \\ \frac{m_1}{m_1+m_2} & -\frac{m_3}{m_1+m_2+m_3} & 0 & -\frac{m_4+m_5}{m_1+m_2+m_3+m_4+m_5} \\ 0 & \frac{m_1+m_2}{m_1+m_2+m_3} & 0 & -\frac{m_4+m_5}{m_1+m_2+m_3+m_4+m_5} \\ 0 & 0 & -\frac{m_5}{m_4+m_5} & \frac{m_1+m_2+m_3}{m_1+m_2+m_3+m_4+m_5} \\ 0 & 0 & \frac{m_4}{m_4+m_5} & \frac{m_1+m_2+m_3}{m_1+m_2+m_3+m_4+m_5} \end{pmatrix}. \quad (31)$$

To describe the spatial wave functions of the baryons and mesons, we use the simple harmonic oscillator (SHO) wave function, i.e.,

$$\begin{aligned} \psi_{n,l,m}(\beta, \mathbf{r}) &= \sqrt{\frac{2n!}{\Gamma(n+l+\frac{3}{2})}} L_n^{l+\frac{1}{2}}(\beta^2 r^2) \beta^{l+\frac{3}{2}} \\ &\times e^{-\frac{\beta^2 r^2}{2}} r^l Y_{lm}(\Omega), \end{aligned} \quad (32)$$

where $Y_{lm}(\Omega)$ is the spherical harmonic function, $L_n^{l+\frac{1}{2}}(x)$ is the associated Laguerre polynomial, n , l , and m are the radial, orbital, and magnetic quantum numbers of the hadron, respectively. The β in Eq. (32) is a parameter of the SHO wave function, and the value of β around 0.4 GeV is a good approximation in the previous theoretical studies [142, 143]. Thus, we also take this value in this work. It should be noted

that the radiative decay width may vary slightly by scanning the value of β from 0.3 to 0.5 GeV. For the hadronic molecular state, since it is a loosely bound state, the obtained spatial wave function (δ -degree of freedom in Fig. 1) is far from the SHO wave function. Thus, we take the precise spatial wave function for the molecular state by solving the Schrödinger equation quantitatively. Furthermore, we use the following equations to expand $e^{-i\mathbf{k}\cdot\mathbf{r}_i}$, i.e.,

$$e^{-i\mathbf{k}\cdot\mathbf{r}_i} = e^{-i\sum_j \alpha_{ij}\mathbf{k}\cdot\mathbf{R}_j} = \prod_j e^{-i\alpha_{ij}\mathbf{k}\cdot\mathbf{R}_j}, \quad (33)$$

$$e^{-i\alpha_{ij}\mathbf{k}\cdot\mathbf{R}_j} = \sum_{l=0}^{\infty} \sum_{m=-l}^l 4\pi(-i)^l j_l(\alpha_{ij}kR_j) Y_{lm}^*(\Omega_{\mathbf{k}}) Y_{lm}(\Omega_{\mathbf{R}_j}). \quad (34)$$

Here, $j_l(x)$ is the spherical Bessel function. In the S -wave scheme, there only exists the $l = 0$ part, which leads to the following relation

$$\begin{aligned} &\langle\psi_{0,0,0}(\beta', \mathbf{R}_j)|e^{-i\alpha_{ij}\mathbf{k}\cdot\mathbf{R}_j}|\psi_{0,0,0}(\beta, \mathbf{R}_j)\rangle \\ &= \int \psi_{0,0,0}(\beta', \mathbf{R}_j) j_0(\alpha_{ij}kR_j) \psi_{0,0,0}(\beta, \mathbf{R}_j) d^3\mathbf{R}_j \\ &= \frac{2\sqrt{2}(\beta'\beta)^{3/2}}{(\beta'^2 + \beta^2)^{3/2}} e^{-\frac{\alpha_{ij}^2 k^2}{2(\beta'^2 + \beta^2)}}. \end{aligned} \quad (35)$$

In the D -wave scheme, we also can take the $l = 0$ part, since we are mainly considering the M1 radiative decay processes. On the other hand, the D -wave component only gives the small contribution in the hadronic molecular states and hardly affects the final result of the radiative decay width, which can be reflected in the following numerical results.

Through the above preparation, we can calculate the radiative decay widths between the $\Xi_c'\bar{D}_s^*$ molecular state with $I(J^P) = 1/2(3/2^-)$ and the $\Xi_c^*\bar{D}_s^*$ molecule with $I(J^P) = 1/2(5/2^-)$ after taking into account the contribution of the spatial wave functions of the initial and final states. Since the radiative decay width depends on the binding energies of the initial and final molecular states, and the $\Xi_c'\bar{D}_s^*$ molecule with $I(J^P) = 1/2(3/2^-)$ and the $\Xi_c^*\bar{D}_s^*$ molecule with $I(J^P) = 1/2(5/2^-)$ are still missing in the experiment. In our concrete calculation, we take three typical binding energies -0.5 MeV, -6.0 MeV, and -12.0 MeV for the initial and final molecules to present the corresponding numerical results. In Table VII, the radiative decay widths between the $\Xi_c'\bar{D}_s^*$ molecular state with $I(J^P) = 1/2(3/2^-)$ and the $\Xi_c^*\bar{D}_s^*$ molecule with $I(J^P) = 1/2(5/2^-)$ are collected, and we discuss these radiative decay widths by performing the single channel, S - D wave mixing, and coupled channel analysis.

As shown in Table VII, the radiative decay width of the $\Xi_c^*\bar{D}_s^*[5/2^-] \rightarrow \Xi_c'\bar{D}_s^*[3/2^-]\gamma$ process with $I_3 = 1/2$ is much smaller than that of the $\Xi_c^*\bar{D}_s^*[5/2^-] \rightarrow \Xi_c^0\bar{D}_s^*[3/2^-]\gamma$ process with $I_3 = -1/2$, which is similar to the radiative decay behavior of the $\Xi_c^{*+} \rightarrow \Xi_c^+\gamma$ and $\Xi_c^{*0} \rightarrow \Xi_c^0\gamma$ processes [117, 130]. Furthermore, the radiative decay widths of these discussed hidden-charm molecular pentaquarks with double strangeness do not change too much with increasing their binding energies [81]. For example, the most significant change of the radiative decay width is the $\Xi_c^*\bar{D}_s^*[5/2^-] \rightarrow \Xi_c'\bar{D}_s^*[3/2^-]\gamma$ process

TABLE VII. The radiative decay widths between the $\Xi_c' \bar{D}_s^*$ molecule with $I(J^P) = 1/2(3/2^-)$ and the $\Xi_c^* \bar{D}_s^*$ molecule with $I(J^P) = 1/2(5/2^-)$ with three different cases: (I) single channel analysis, (II) S - D wave mixing analysis, and (III) coupled channel analysis. Here, the radiative decay width is in units of keV.

I_3	Case I	Case II	Case III
1/2	0.041, 0.045, 0.046	0.041, 0.045, 0.045	0.012, 0.003, 0.017
-1/2	1.333, 1.460, 1.469	1.327, 1.463, 1.467	1.329, 1.464, 1.462

with $I_3 = -1/2$ when performing the coupled channel analysis, which is less than 0.02 keV. In addition, the D -wave component hardly affects the radiative decay widths of the $\Xi_c^* \bar{D}_s^* |5/2^- \rangle \rightarrow \Xi_c' \bar{D}_s^* |3/2^- \rangle \gamma$ process.

III. THE ELECTROMAGNETIC PROPERTIES OF THE $\Omega_c^{(*)} \bar{D}_s^*$ MOLECULAR STATES

In our previous study [82], we predicted the existences of the $\Omega_c \bar{D}_s^*$ molecular state with $I(J^P) = 0(3/2^-)$ and the $\Omega_c^* \bar{D}_s^*$ molecular state with $I(J^P) = 0(5/2^-)$. In order to reflect the inner structures of the $\Omega_c \bar{D}_s^*$ molecule with $I(J^P) = 0(3/2^-)$ and the $\Omega_c^* \bar{D}_s^*$ molecular state with $I(J^P) = 0(5/2^-)$, it is essential to provide their electromagnetic properties. Within the constituent quark model, the procedure for calculating the magnetic moments and the transition magnetic moment of the $\Omega_c^{(*)} \bar{D}_s^*$ molecular states is same as that of the $\Xi_c^{(*)} \bar{D}_s^*$ molecular states. The flavor wave functions of the $\Omega_c^{(*)0}$ baryons are written as ssc , and their corresponding spin wave functions $|S, S_3\rangle$ can be expressed as

$$\Omega_c : \begin{cases} \left| \frac{1}{2}, \frac{1}{2} \right\rangle = \frac{1}{\sqrt{6}} (2 \uparrow \uparrow \downarrow - \downarrow \uparrow \uparrow - \uparrow \downarrow \uparrow) \\ \left| \frac{1}{2}, -\frac{1}{2} \right\rangle = \frac{1}{\sqrt{6}} (\downarrow \uparrow \downarrow + \uparrow \downarrow \downarrow - 2 \downarrow \uparrow \uparrow) \end{cases},$$

$$\Omega_c^* : \begin{cases} \left| \frac{3}{2}, \frac{3}{2} \right\rangle = \uparrow \uparrow \uparrow \\ \left| \frac{3}{2}, \frac{1}{2} \right\rangle = \frac{1}{\sqrt{3}} (\downarrow \uparrow \uparrow + \uparrow \downarrow \uparrow + \uparrow \uparrow \downarrow) \\ \left| \frac{3}{2}, -\frac{1}{2} \right\rangle = \frac{1}{\sqrt{3}} (\downarrow \downarrow \uparrow + \uparrow \downarrow \downarrow + \downarrow \uparrow \downarrow) \\ \left| \frac{3}{2}, -\frac{3}{2} \right\rangle = \downarrow \downarrow \downarrow \end{cases}.$$

In Table VIII, the results for the magnetic moments and the transition magnetic moment of the $\Omega_c^{(*)}$ baryons are collected. Furthermore, we compare these numerical results with other theoretical predictions [103, 104, 115, 117, 129], where our obtained results are comparable with other theoretical values [103, 104, 115, 117, 129]. Interestingly, the magnetic moments of the Ω_c^0 and Ω_c^{*0} are very close to each other, which is similar to the case of the magnetic moments of the Ξ_c^{*0} and Ξ_c^{*0} .

And then, we can study the magnetic moments, the transition magnetic moment, and the radiative decay width of the

TABLE VIII. The magnetic moments and the transition magnetic moment of the $\Omega_c^{(*)}$ baryons. Here, the magnetic moment and the transition magnetic moment are in units of μ_N , while the square brackets represent the expressions of their magnetic moments and transition magnetic moment in the second column.

Quantities	Our results	Other results
$\mu_{\Omega_c^0}$	$-1.051 \left[\frac{4}{3}\mu_s - \frac{1}{3}\mu_c \right]$	-1.127 [115], -0.960 [129]
$\mu_{\Omega_c^{*0}}$	$-1.018 [2\mu_s + \mu_c]$	-1.127 [115], -0.936 [117]
$\mu_{\Omega_c^{*0} \rightarrow \Omega_c^0}$	$-1.006 \left[\frac{2\sqrt{2}}{3}(\mu_s - \mu_c) \right]$	-0.960 [104], -1.128 [103]

$\Omega_c \bar{D}_s^*$ molecular state with $I(J^P) = 0(3/2^-)$ and the $\Omega_c^* \bar{D}_s^*$ molecular state with $I(J^P) = 0(5/2^-)$. Here, the involved flavor wave functions $|I, I_3\rangle$ are expressed as $|0, 0\rangle = |\Omega_c^{(*)0} \bar{D}_s^{*-}\rangle$, where I and I_3 are the isospins and isospin third components of the $\Omega_c^{(*)} \bar{D}_s^*$ systems, respectively. Their spin wave functions $|S, S_3\rangle$ can be constructed by the coupling of the spin wave functions of the constitute hadrons, i.e.,

$$\Omega_c \bar{D}_s^* : |S, S_3\rangle = \sum_{S_{\Omega_c}, S_{\bar{D}_s^*}} C_{S_{\Omega_c}, S_{\bar{D}_s^*}}^{SS_3} \left| \frac{1}{2}, S_{\Omega_c} \right\rangle \left| 1, S_{\bar{D}_s^*} \right\rangle,$$

$$\Omega_c^* \bar{D}_s^* : |S, S_3\rangle = \sum_{S_{\Omega_c^*}, S_{\bar{D}_s^*}} C_{S_{\Omega_c^*}, S_{\bar{D}_s^*}}^{SS_3} \left| \frac{3}{2}, S_{\Omega_c^*} \right\rangle \left| 1, S_{\bar{D}_s^*} \right\rangle.$$

Here, S and S_3 stand for the spins and spin third components of the $\Omega_c^{(*)} \bar{D}_s^*$ systems, respectively. The notations S_{Ω_c} , $S_{\Omega_c^*}$, and $S_{\bar{D}_s^*}$ denote the third components of the spins of the Ω_c , Ω_c^* , and \bar{D}_s^* , respectively.

Similar to the case for the hidden-charm molecular pentaquarks with double strangeness, the study of the electromagnetic properties of the $\Omega_c \bar{D}_s^*$ molecular state with $I(J^P) = 0(3/2^-)$ and the $\Omega_c^* \bar{D}_s^*$ molecular state with $I(J^P) = 0(5/2^-)$ is carried out when the single channel analysis, the S - D wave mixing analysis, and the coupled channel analysis are included in the calculation one by one. For the case of considering the S - D wave mixing effect, the allowed S -wave and D -wave channels $|^{2S+1}L_J\rangle$ for the $\Omega_c \bar{D}_s^*$ molecular state with $I(J^P) = 0(3/2^-)$ and the $\Omega_c^* \bar{D}_s^*$ molecular state with $I(J^P) = 0(5/2^-)$ are [82]

$$\Omega_c \bar{D}_s^* |3/2^- \rangle : |^4S_{3/2}\rangle, |^2D_{3/2}\rangle, |^4D_{3/2}\rangle,$$

$$\Omega_c^* \bar{D}_s^* |5/2^- \rangle : |^6S_{5/2}\rangle, |^2D_{5/2}\rangle, |^4D_{5/2}\rangle, |^6D_{5/2}\rangle.$$

In addition, we can further consider the contribution of the coupled channel effect for the $\Omega_c \bar{D}_s^*$ molecular state with $I(J^P) = 0(3/2^-)$ [82].

In Table IX, we present the numerical results of the electromagnetic properties of the $\Omega_c \bar{D}_s^*$ molecular state with $I(J^P) = 0(3/2^-)$ and the $\Omega_c^* \bar{D}_s^*$ molecular state with $I(J^P) = 0(5/2^-)$ by performing the single channel, S - D wave mixing, and coupled channel analysis, respectively. Here, we take three typical binding energies -0.5 MeV, -6.0 MeV, and -12.0 MeV for the discussed molecular states to present their magnetic moments, transition magnetic moments, and radiative decay widths. For the radiative decay width of the $\Omega_c^* \bar{D}_s^* |5/2^- \rangle \rightarrow$

$\Omega_c \bar{D}_s^* |3/2^- \rangle \gamma$ process, we also consider the contribution of the spatial wave functions of the initial and final states.

From Table IX, we can find several interesting results:

1. Since the magnetic moments of the Ω_c^0 and Ω_c^{*0} are very close to each other, the magnetic moments of the $\Omega_c \bar{D}_s^*$ molecular state with $I(J^P) = 0(3/2^-)$ and the $\Omega_c^* \bar{D}_s^*$ molecular state with $I(J^P) = 0(5/2^-)$ are almost the same. In addition, the radiative decay width of the $\Omega_c \bar{D}_s^* |5/2^- \rangle \rightarrow \Omega_c \bar{D}_s^* |3/2^- \rangle \gamma$ process is about 1.00 keV.
2. The S - D wave mixing effect is not obvious to the magnetic moments, the transition magnetic moment, and the radiative decay width of the $\Omega_c \bar{D}_s^*$ molecular state with $I(J^P) = 0(3/2^-)$ and the $\Omega_c^* \bar{D}_s^*$ molecular state with $I(J^P) = 0(5/2^-)$, since the changes of their magnetic moments and transition magnetic moment are smaller than $0.004 \mu_N$ after taking into account the contribution of the D -wave channels. The main reason is that the S - D wave mixing effect can be ignored for the formation of the $\Omega_c \bar{D}_s^*$ molecular state with $I(J^P) = 0(3/2^-)$ and the $\Omega_c^* \bar{D}_s^*$ molecular state with $I(J^P) = 0(5/2^-)$ [82].
3. The coupled channel effect has an influence on the electromagnetic properties of these discussed hidden-charm molecular pentaquarks with triple strangeness, where the changes of their magnetic moments and transition magnetic moment are smaller than $0.09 \mu_N$.

Furthermore, the electromagnetic properties of these discussed hidden-charm molecular pentaquarks with double strangeness and triple strangeness show several similarities. In particular, the numerical results of $\mu_{\Xi_c' \bar{D}_s^* |3/2^- \rangle}$, $\mu_{\Xi_c' \bar{D}_s^* |5/2^- \rangle}$, and $\mu_{\Xi_c' \bar{D}_s^* |5/2^- \rangle \rightarrow \Xi_c' \bar{D}_s^* |3/2^- \rangle}$ with $I_3 = -1/2$ are close to $\mu_{\Omega_c \bar{D}_s^* |3/2^- \rangle}$, $\mu_{\Omega_c^* \bar{D}_s^* |5/2^- \rangle}$, and $\mu_{\Omega_c^* \bar{D}_s^* |5/2^- \rangle \rightarrow \Omega_c \bar{D}_s^* |3/2^- \rangle}$ with $I_3 = 0$, respectively, since the magnetic moments and the transition magnetic moment of the $\Xi_c^{(*)0}$ baryons are similar to those of the $\Omega_c^{(*)0}$ baryons.

IV. SUMMARY

Since the discovery of the hidden-charm pentaquark structures $P_c(4380)$ and $P_c(4450)$ by LHCb in 2015 [23], the study of the hidden-charm molecular pentaquarks has become a focused topic in hadron physics [7–11, 14, 15, 17, 19, 21, 22]. In recent years, remarkable progress has been made on both the theoretical and experimental sides, where these topics have been simultaneously explored around the mass spectra, decay behavior, and production mechanisms of different types of hidden-charm molecular pentaquarks, which deepen our understanding of the nature of hidden-charm pentaquarks. Obviously, this is not the end of the story.

In Refs. [81, 82], the Lanzhou group once predicted the existence of the hidden-charm molecular pentaquark candidates with double strangeness and triple strangeness by discussing the $\Xi_c^{(*)} \bar{D}_s^{(*)}$ and $\Omega_c^{(*)} \bar{D}_s^{(*)}$ interactions, where their mass spectra were given. Facing these predicted hidden-charm molecular pentaquark candidates with double strangeness and triple

strangeness, in this work we propose to study their electromagnetic properties including the magnetic moments, the transition magnetic moments, and the radiative decay behavior, which are important physical quantities reflecting their inner structures. In the concrete investigation, various effects including the S - D wave mixing effect and the coupled channel effect are considered.

In summary, the present investigation is only a starting point for the study of the electromagnetic properties of the $\Xi_c^{(*)} \bar{D}_s^*$ and $\Omega_c^{(*)} \bar{D}_s^*$ molecular states. Further theoretical studies by different approaches and models around this topic are encouraged. Of course, experimental measurements of the electromagnetic properties of these discussed pentaquarks will be a challenging task in the future.

As the crucial information reflecting the inner structure of hadrons, the study of their electromagnetic properties can be used to distinguish their spin-parity quantum numbers and configurations. It is worthwhile to study the magnetic moments of non-molecular hidden-charm pentaquarks with double or triple strangeness in the future, which will help to distinguish the nature of these pentaquarks. Since our knowledge of the electromagnetic properties of the compact hidden-charm pentaquarks with double strangeness and triple strangeness is still lacking, further experimental and theoretical investigations of these discussed exotic states are encouraged, which may provide valuable information for the construction of the cluster composed of the hidden-charm pentaquarks with double strangeness and triple strangeness.

ACKNOWLEDGEMENT

This work is supported by the China National Funds for Distinguished Young Scientists under Grant No. 11825503, National Key Research and Development Program of China under Contract No. 2020YFA0406400, the 111 Project under Grant No. B20063, and the National Natural Science Foundation of China under Grant Nos. 12175091, 11965016, 12047501, and 12247155. F.L.W is also supported by the China Postdoctoral Science Foundation under Grant No. 2022M721440.

Appendix A: The derivation of the formula for the radiative decay width related to the transition magnetic moment

In the following, we derive the formula for the radiative decay width related to the transition magnetic moment. According to Ref. [141], the standard helicity transition amplitude $\mathcal{A}_{J_f}^M$ for the magnetic operators between the initial state $|J_i, J_{iz}\rangle$ and the final state $|J_f, J_{fz}\rangle$ can be written as

$$\mathcal{A}_{J_f}^M = i \sqrt{\frac{E_\gamma}{2}} \langle J_f, J_{fz} | \sum_j \frac{e_j}{2m_j} \hat{\sigma}_j \cdot (\epsilon \times \hat{k}) | J_i, J_{iz} \rangle, \quad (\text{A1})$$

where E_γ is the energy of the emitted photon. Here, we need to specify that the spatial wave function of the emitted photon $e^{-ik \cdot r_i}$ was not included in the above expression. For the

TABLE IX. The magnetic moments, the transition magnetic moment, and the radiative decay width of the $\Omega_c \bar{D}_s^*$ molecular state with $I(J^P) = 0(3/2^-)$ and the $\Omega_c^* \bar{D}_s^*$ molecular state with $I(J^P) = 0(5/2^-)$ by performing the single channel, S - D wave mixing, and coupled channel analysis, respectively.

Physical quantities	Single channel analysis	S - D wave mixing analysis	Coupled channel analysis
$\mu_{\Omega_c \bar{D}_s^* [3/2^-]}$	$-2.118 \mu_N$	$-2.117 \mu_N, -2.117 \mu_N, -2.117 \mu_N$	$-2.152 \mu_N, -2.190 \mu_N, -2.199 \mu_N$
$\mu_{\Omega_c^* \bar{D}_s^* [5/2^-]}$	$-2.085 \mu_N$	$-2.084 \mu_N, -2.084 \mu_N, -2.084 \mu_N$	/
$\mu_{\Omega_c^* \bar{D}_s^* [5/2^-] \rightarrow \Omega_c \bar{D}_s^* [3/2^-]}$	$-0.780 \mu_N$	$-0.778 \mu_N, -0.776 \mu_N, -0.776 \mu_N$	$-0.787 \mu_N, -0.795 \mu_N, -0.796 \mu_N$
$\Gamma_{\Omega_c^* \bar{D}_s^* [5/2^-] \rightarrow \Omega_c \bar{D}_s^* [3/2^-] \gamma}$	1.483 keV, 1.603 keV, 1.608 keV	1.463 keV, 1.600 keV, 1.604 keV	1.500 keV, 1.680 keV, 1.692 keV

convenience of calculation, we choose the Pauli spin operator along the z axial, the above expression can be simplified as

$$\mathcal{A}_{J_{fz}}^M = i \sqrt{\frac{E_\gamma}{2}} \langle J_f, J_{fz} | \hat{\mu}_z | J_i, J_{iz} \rangle, \quad (\text{A2})$$

where $\hat{\mu}_z = \sum_j \frac{e_j}{2M_j} \hat{\sigma}_{zj}$. Furthermore, the radiative decay widths can be given by [141]

$$\begin{aligned} \Gamma &= \frac{|\mathbf{k}|^2}{\pi} \frac{2}{2J_i + 1} \sum_{J_{fz}} |\mathcal{A}_{J_{fz}}^M|^2 \\ &= \frac{|\mathbf{k}|^2}{\pi} \frac{2}{2J_i + 1} \sum_{J_{fz}} \frac{E_\gamma}{2} |\langle J_f, J_{fz} | \hat{\mu}_z | J_i, J_{iz} \rangle|^2 \\ &= \alpha_{\text{EM}} \frac{E_\gamma^3}{M_P^2} \frac{1}{2J_i + 1} \frac{\sum_{J_{fz}} |\langle J_f, J_{fz} | \hat{\mu}_z | J_i, J_{iz} \rangle|^2}{\mu_N^2}. \end{aligned} \quad (\text{A3})$$

In the above expression, we use $\alpha_{\text{EM}} = e^2/4\pi$ and $\mu_N = e/2M_P$. Thus, the radiative decay width $\Gamma_{H \rightarrow H' \gamma}$ of the radiative decay process $H \rightarrow H' \gamma$ can be expressed as¹

$$\Gamma_{H \rightarrow H' \gamma} = \alpha_{\text{EM}} \frac{E_\gamma^3}{M_P^2} \frac{1}{2J_H + 1} \sum_{J_{H'z}} \left(\frac{\langle J_{H'}, J_{H'z} | \hat{\mu}_z | J_H, J_{Hz} \rangle}{\mu_N} \right)^2. \quad (\text{A4})$$

If considering the relation $\langle J_{H'}, J_{H'z} | \hat{\mu}_z | J_H, J_{Hz} \rangle = \mu_{H \rightarrow H'} J_{H^{(\gamma)z}} / J_{H^{(\gamma)}}$, the above expression can be simplified as

$$\Gamma_{H \rightarrow H' \gamma} = \alpha_{\text{EM}} \frac{E_\gamma^3}{M_P^2} \frac{J_H + 1}{3J_H} \left(\frac{\mu_{H \rightarrow H'}}{\mu_N} \right)^2, \quad (\text{A5})$$

$$\Gamma_{H \rightarrow H' \gamma} = \alpha_{\text{EM}} \frac{E_\gamma^3}{M_P^2} \frac{(J_{H'} + 1)(2J_{H'} + 1)}{3(2J_H + 1)J_{H'}} \left(\frac{\mu_{H \rightarrow H'}}{\mu_N} \right)^2, \quad (\text{A6})$$

when $J_H \leq J_{H'}$ and $J_H > J_{H'}$, respectively.

- [1] C. Amsler and N. A. Tornqvist, Mesons beyond the naive quark model, Phys. Rept. **389**, 61-117 (2004).
- [2] E. S. Swanson, The New heavy mesons: A Status report, Phys. Rept. **429**, 243-305 (2006).
- [3] S. Godfrey and S. L. Olsen, The Exotic XYZ Charmonium-like Mesons, Ann. Rev. Nucl. Part. Sci. **58**, 51-73 (2008).
- [4] N. Drenska, R. Faccini, F. Piccinini, A. Polosa, F. Renga and C. Sabelli, New Hadronic Spectroscopy, Riv. Nuovo Cim. **33**, no.11, 633-712 (2010).
- [5] G. V. Pakhlova, P. N. Pakhlov and S. I. Eidelman, Exotic charmonium, Phys. Usp. **53**, 219-241 (2010).
- [6] R. Faccini, A. Pilloni and A. D. Polosa, Exotic Heavy Quarkonium Spectroscopy: A Mini-review, Mod. Phys. Lett. A **27**, 1230025 (2012).
- [7] X. Liu, An overview of XYZ new particles, Chin. Sci. Bull. **59**, 3815 (2014).
- [8] A. Hosaka, T. Iijima, K. Miyabayashi, Y. Sakai, and S. Yasui, Exotic hadrons with heavy flavors: X , Y , Z , and related states, Prog. Theor. Exp. Phys. **2016**, 062C01 (2016).

- [9] H. X. Chen, W. Chen, X. Liu, and S. L. Zhu, The hidden-charm pentaquark and tetraquark states, Phys. Rep. **639**, 1 (2016).
- [10] J. M. Richard, Exotic hadrons: review and perspectives, Few Body Syst. **57**, 1185-1212 (2016).
- [11] R. F. Lebed, R. E. Mitchell and E. S. Swanson, Heavy-Quark QCD Exotica, Prog. Part. Nucl. Phys. **93** (2017), 143-194.
- [12] A. Ali, J. S. Lange and S. Stone, Exotics: Heavy Pentaquarks and Tetraquarks, Prog. Part. Nucl. Phys. **97**, 123-198 (2017).
- [13] Y. Dong, A. Faessler and V. E. Lyubovitskij, Description of heavy exotic resonances as molecular states using phenomenological Lagrangians, Prog. Part. Nucl. Phys. **94**, 282-310 (2017).
- [14] S. L. Olsen, T. Skwarnicki, and D. Zieminska, Nonstandard heavy mesons and baryons: Experimental evidence, Rev. Mod. Phys. **90**, 015003 (2018).
- [15] F. K. Guo, C. Hanhart, U. G. Meißner, Q. Wang, Q. Zhao, and B. S. Zou, Hadronic molecules, Rev. Mod. Phys. **90**, 015004 (2018).
- [16] C. Z. Yuan, The XYZ states revisited, Int. J. Mod. Phys. A **33**, no.21, 1830018 (2018).
- [17] Y. R. Liu, H. X. Chen, W. Chen, X. Liu, and S. L. Zhu, Pentaquark and tetraquark states, Prog. Part. Nucl. Phys. **107**, 237 (2019).
- [18] R. M. Albuquerque, J. M. Dias, K. P. Khemchandani, A. Martínez Torres, F. S. Navarra, M. Nielsen and

¹ Here, we need to specify that the formulas for the radiative decay width related to the transition magnetic moment in Refs. [92, 98] can be only used for several special decay processes, such as the $1/2 \rightarrow 1/2 + \gamma$ process, the $3/2 \rightarrow 1/2 + \gamma$ process, and so on.

- C. M. Zanetti, QCD sum rules approach to the X , Y and Z states, *J. Phys. G* **46**, no.9, 093002 (2019).
- [19] N. Brambilla, S. Eidelman, C. Hanhart, A. Nefediev, C. P. Shen, C. E. Thomas, A. Vairo, and C. Z. Yuan, The XYZ states: Experimental and theoretical status and perspectives, *Phys. Rep.* **873**, 1 (2020).
- [20] Y. Yamaguchi, A. Hosaka, S. Takeuchi and M. Takizawa, Heavy hadronic molecules with pion exchange and quark core couplings: a guide for practitioners, *J. Phys. G* **47**, no.5, 053001 (2020).
- [21] L. Meng, B. Wang, G. J. Wang and S. L. Zhu, Chiral perturbation theory for heavy hadrons and chiral effective field theory for heavy hadronic molecules, arXiv:2204.08716.
- [22] H. X. Chen, W. Chen, X. Liu, Y. R. Liu and S. L. Zhu, An updated review of the new hadron states, *Rept. Prog. Phys.* **86**, no.2, 026201 (2023).
- [23] R. Aaij *et al.* (LHCb Collaboration), Observation of J/ψ Resonances Consistent with Pentaquark States in $\Lambda_b^0 \rightarrow J/\psi K^- p$ Decays, *Phys. Rev. Lett.* **115**, 072001 (2015).
- [24] R. Aaij *et al.* (LHCb Collaboration), Observation of a Narrow Pentaquark State, $P_c(4312)^+$, and of Two-Peak Structure of the $P_c(4450)^+$, *Phys. Rev. Lett.* **122**, 222001 (2019).
- [25] J. J. Wu, R. Molina, E. Oset and B. S. Zou, Prediction of narrow N^* and Λ^* resonances with hidden charm above 4 GeV, *Phys. Rev. Lett.* **105**, 232001 (2010).
- [26] W. L. Wang, F. Huang, Z. Y. Zhang, and B. S. Zou, $\Sigma_c \bar{D}$ and $\Lambda_c \bar{D}$ states in a chiral quark model, *Phys. Rev. C* **84**, 015203 (2011).
- [27] Z. C. Yang, Z. F. Sun, J. He, X. Liu, and S. L. Zhu, The possible hidden-charm molecular baryons composed of anti-charmed meson and charmed baryon, *Chin. Phys. C* **36**, 6 (2012).
- [28] J. J. Wu, T.-S. H. Lee, and B. S. Zou, Nucleon resonances with hidden charm in coupled-channel Models, *Phys. Rev. C* **85**, 044002 (2012).
- [29] X. Q. Li and X. Liu, A possible global group structure for exotic states, *Eur. Phys. J. C* **74**, 3198 (2014).
- [30] R. Chen, X. Liu, X. Q. Li, and S. L. Zhu, Identifying Exotic Hidden-Charm Pentaquarks, *Phys. Rev. Lett.* **115**, 132002 (2015).
- [31] M. Karliner and J. L. Rosner, New Exotic Meson and Baryon Resonances from Doubly-Heavy Hadronic Molecules, *Phys. Rev. Lett.* **115**, 122001 (2015).
- [32] R. Aaij *et al.* (LHCb Collaboration), Evidence of a $J/\psi\Lambda$ structure and observation of excited Ξ^- states in the $\Xi_b^- \rightarrow J/\psi\Lambda K^-$ decay, *Sci. Bull.* **66**, 1278-1287 (2021).
- [33] L. Collaboration (LHCb Collaboration), Observation of a $J/\psi\Lambda$ resonance consistent with a strange pentaquark candidate in $B^- \rightarrow J/\psi\Lambda\bar{p}$ decays, arXiv:2210.10346.
- [34] J. Hofmann and M. F. M. Lutz, Coupled-channel study of crypto-exotic baryons with charm, *Nucl. Phys. A* **763**, 90 (2005).
- [35] J. J. Wu, R. Molina, E. Oset and B. S. Zou, Dynamically generated N^* and Λ^* resonances in the hidden charm sector around 4.3 GeV, *Phys. Rev. C* **84**, 015202 (2011).
- [36] V. V. Anisovich, M. A. Matveev, J. Nyiri, A. V. Sarantsev, and A. N. Semenova, Nonstrange and strange pentaquarks with hidden charm, *Int. J. Mod. Phys. A* **30**, 1550190 (2015).
- [37] Z. G. Wang, Analysis of the $\frac{1}{2}^\pm$ pentaquark states in the diquark-diquark-antiquark model with QCD sum rules, *Eur. Phys. J. C* **76**, 142 (2016).
- [38] A. Feijoo, V. K. Magas, A. Ramos, and E. Oset, A hidden-charm $S = -1$ pentaquark from the decay of Λ_b into $J/\psi\eta\Lambda$ states, *Eur. Phys. J. C* **76**, no. 8, 446 (2016).
- [39] J. X. Lu, E. Wang, J. J. Xie, L. S. Geng, and E. Oset, The $\Lambda_b \rightarrow J/\psi K^0 \Lambda$ reaction and a hidden-charm pentaquark state with strangeness, *Phys. Rev. D* **93**, 094009 (2016).
- [40] H. X. Chen, L. S. Geng, W. H. Liang, E. Oset, E. Wang, and J. J. Xie, Looking for a hidden-charm pentaquark state with strangeness $S = -1$ from Ξ_b^- decay into $J/\psi K^- \Lambda$, *Phys. Rev. C* **93**, 065203 (2016).
- [41] R. Chen, J. He, and X. Liu, Possible strange hidden-charm pentaquarks from $\Sigma_c^{(*)} \bar{D}_s^*$ and $\Xi_c^{(*)} \bar{D}^*$ interactions, *Chin. Phys. C* **41**, 103105 (2017).
- [42] X. Z. Weng, X. L. Chen, W. Z. Deng and S. L. Zhu, Hidden-charm pentaquarks and P_c states, *Phys. Rev. D* **100**, 016014 (2019).
- [43] C. W. Xiao, J. Nieves, and E. Oset, Prediction of hidden charm strange molecular baryon states with heavy quark spin symmetry, *Phys. Lett. B* **799**, 135051 (2019).
- [44] C. W. Shen, H. J. Jing, F. K. Guo, and J. J. Wu, Exploring possible triangle singularities in the $\Xi_b^- \rightarrow K^- J/\psi \Lambda$ decay, *Symmetry* **12**, 1611 (2020).
- [45] B. Wang, L. Meng, and S. L. Zhu, Spectrum of the strange hidden charm molecular pentaquarks in chiral effective field theory, *Phys. Rev. D* **101**, 034018 (2020).
- [46] Q. Zhang, B. R. He, and J. L. Ping, Pentaquarks with the $qq\bar{s}\bar{Q}Q$ configuration in the Chiral Quark Model, arXiv:2006.01042.
- [47] H. X. Chen, W. Chen, X. Liu, and X. H. Liu, Establishing the first hidden-charm pentaquark with strangeness, *Eur. Phys. J. C* **81**, 409 (2021).
- [48] F. Z. Peng, M. J. Yan, M. Sánchez Sánchez, and M. P. Valderama, The $P_{cs}(4459)$ pentaquark from a combined effective field theory and phenomenological perspectives, *Eur. Phys. J. C* **81**, 666 (2021).
- [49] R. Chen, Can the newly reported $P_{cs}(4459)$ be a strange hidden-charm $\Xi_c \bar{D}^*$ molecular pentaquark?, *Phys. Rev. D* **103**, 054007 (2021).
- [50] H. X. Chen, Hidden-charm pentaquark states through the current algebra: From their productions to decays, *Chin. Phys. C* **46**, 093105 (2022).
- [51] M. Z. Liu, Y. W. Pan, and L. S. Geng, Can discovery of hidden charm strange pentaquark states help determine the spins of $P_c(4440)$ and $P_c(4457)$?, *Phys. Rev. D* **103**, 034003 (2021).
- [52] C. W. Xiao, J. J. Wu and B. S. Zou, Molecular nature of $P_{cs}(4459)$ and its heavy quark spin partners, *Phys. Rev. D* **103**, 054016 (2021).
- [53] M. L. Du, Z. H. Guo and J. A. Oller, Insights into the nature of the $P_{cs}(4459)$, *Phys. Rev. D* **104**, 114034 (2021).
- [54] J. T. Zhu, L. Q. Song and J. He, $P_{cs}(4459)$ and other possible molecular states from $\Xi_c^{(*)} \bar{D}^{(*)}$ and $\Xi_c' \bar{D}^{(*)}$ interactions, *Phys. Rev. D* **103**, 074007 (2021).
- [55] X. K. Dong, F. K. Guo and B. S. Zou, A survey of heavy-antiheavy hadronic molecules, *Progr. Phys.* **41**, 65-93 (2021).
- [56] K. Chen, R. Chen, L. Meng, B. Wang and S. L. Zhu, Systematics of the heavy flavor hadronic molecules, *Eur. Phys. J. C* **82**, 581 (2022).
- [57] R. Chen and X. Liu, Mass behavior of hidden-charm open-strange pentaquarks inspired by the established P_c molecular states, *Phys. Rev. D* **105**, 014029 (2022).
- [58] K. Chen, B. Wang and S. L. Zhu, Heavy flavor molecular states with strangeness, *Phys. Rev. D* **105**, 096004 (2022).
- [59] X. Hu and J. Ping, Investigation of hidden-charm pentaquarks with strangeness $S = -1$, *Eur. Phys. J. C* **82**, 118 (2022).
- [60] X. W. Wang and Z. G. Wang, Analysis of $P_{cs}(4338)$ and related pentaquark molecular states via QCD sum rules*, *Chin.*

- Phys. C **47**, no.1, 013109 (2023).
- [61] M. Karliner and J. R. Rosner, strange pentaquarks, Phys. Rev. D **106**, 036024 (2022).
- [62] F. L. Wang and X. Liu, Emergence of molecular-type characteristic spectrum of hidden-charm pentaquark with strangeness embodied in the $P_{\psi s}^{\Lambda}(4338)$ and $P_{cs}(4459)$, Phys. Lett. B **835**, 137583 (2022).
- [63] M. J. Yan, F. Z. Peng, M. S. Sánchez and M. Pavon Valderama, The $P_{\psi s}^{\Lambda}(4338)$ pentaquark and its partners in the molecular picture, arXiv:2207.11144.
- [64] L. Meng, B. Wang and S. L. Zhu, Double thresholds distort the line shapes of the $P\psi\Lambda(4338)0$ resonance, Phys. Rev. D **107**, no.1, 1 (2023).
- [65] K. Azizi, Y. Sarac and H. Sundu, Investigation of $P_{cs}(4459)^0$ pentaquark via its strong decay to $\Lambda J/\Psi$, Phys. Rev. D **103**, no.9, 094033 (2021).
- [66] R. Chen, Strong decays of the newly $P_{cs}(4459)$ as a strange hidden-charm $\Xi_c \bar{D}^*$ molecule, Eur. Phys. J. C **81**, no.2, 122 (2021).
- [67] S. Clymton, H. J. Kim and H. C. Kim, Production of hidden-charm strange pentaquarks Pcs from the $K^- p \rightarrow J/\psi \Lambda$ reaction, Phys. Rev. D **104**, no.1, 014023 (2021).
- [68] B. S. Zou, Building up the spectrum of pentaquark states as hadronic molecules, Sci. Bull. **66**, 1258 (2021).
- [69] J. X. Lu, M. Z. Liu, R. X. Shi and L. S. Geng, Understanding $P_{cs}(4459)$ as a hadronic molecule in the $\Xi_b^- \rightarrow J/\psi \Lambda K^-$ decay, Phys. Rev. D **104**, no.3, 034022 (2021).
- [70] J. Ferretti and E. Santopinto, The new $P_{cs}(4459)$, $Z_{cs}(3985)$, $Z_{cs}(4000)$ and $Z_{cs}(4220)$ and the possible emergence of flavor pentaquark octets and tetraquark nonets, Sci. Bull. **67**, 1209 (2022).
- [71] E. Y. Paryev, Regarding the possibility to observe the LHCb hidden-charm strange pentaquark $P_{cs}(4459)^0$ in antikaon-induced J/ψ meson production on protons and nuclei near the $J/\psi \Lambda$ production threshold, Nucl. Phys. A **1023**, 122452 (2022).
- [72] S. X. Nakamura and J. J. Wu, Pole determination of $P_{\psi s}^{\Lambda}(4338)$ and possible $P_{\psi s}^{\Lambda}(4255)$ in $B^- \rightarrow J/\psi \Lambda \bar{p}$, arXiv:2208.11995.
- [73] A. Giachino, A. Hosaka, E. Santopinto, S. Takeuchi, M. Takizawa and Y. Yamaguchi, Rich structure of the hidden-charm pentaquarks near threshold regions, arXiv:2209.10413.
- [74] J. A. M. Valera, I. V. K. Magas and A. Ramos, Double strangeness molecular-type pentaquarks from coupled channel dynamics, arXiv:2210.02792.
- [75] P. G. Ortega, D. R. Entem and F. Fernandez, Strange hidden-charm $P_{\psi s}^{\Lambda}(4459)$ and $P_{\psi s}^{\Lambda}(4338)$ pentaquarks and additional $P_{\psi s}^{\Lambda}$, $P_{\psi s}^{\Sigma}$ and $P_{\psi ss}^N$ candidates in a quark model approach, Phys. Lett. B **838**, 137747 (2023).
- [76] K. Chen, Z. Y. Lin and S. L. Zhu, Comparison between the P_{ψ}^N and $P_{\psi s}^{\Lambda}$ systems, Phys. Rev. D **106**, no.11, 116017 (2022).
- [77] J. T. Zhu, S. Y. Kong and J. He, $P_{\psi s}^{\Lambda}(4459)$ and $P_{\psi s}^{\Lambda}(4338)$ as molecular states in $J/\psi \Lambda$ invariant mass spectra, arXiv:2211.06232.
- [78] Z. Y. Yang, F. Z. Peng, M. J. Yan, M. Sánchez Sánchez and M. Pavon Valderrama, Molecular P_{ψ} pentaquarks from light-meson exchange saturation, arXiv:2211.08211.
- [79] H. Garcilazo and A. Valcarce, Hidden-flavor pentaquarks, Phys. Rev. D **106**, no.11, 114012 (2022).
- [80] A. Feijoo, W. F. Wang, C. W. Xiao, J. J. Wu, E. Oset, J. Nieves and B. S. Zou, A new look at the P_{cs} states from a molecular perspective, arXiv:2212.12223.
- [81] F. L. Wang, R. Chen, and X. Liu, Prediction of hidden-charm pentaquarks with double strangeness, Phys. Rev. D **103**, 034014 (2021).
- [82] F. L. Wang, X. D. Yang, R. Chen and X. Liu, Hidden-charm pentaquarks with triple strangeness due to the $\Omega_c^{(*)} \bar{D}_s^{(*)}$ interactions, Phys. Rev. D **103**, 054025 (2021).
- [83] K. Azizi, Y. Sarac and H. Sundu, Investigation of hidden-charm double strange pentaquark candidate $P_{c\bar{s}s}$ via its mass and strong decays, Eur. Phys. J. C **82**, no.6, 543 (2022).
- [84] K. Azizi, Y. Sarac and H. Sundu, Investigation of a candidate spin- $\frac{1}{2}$ hidden-charm triple strange pentaquark state $P_{c\bar{s}s}s$, Phys. Rev. D **107**, no.1, 014023 (2023).
- [85] F. Schlumpf, Magnetic moments of the baryon decuplet in a relativistic quark model, Phys. Rev. D **48**, 4478-4480 (1993).
- [86] S. Kumar, R. Dhir and R. C. Verma, Magnetic moments of charm baryons using effective mass and screened charge of quarks, J. Phys. G **31**, 141-147 (2005).
- [87] G. Ramalho, K. Tsushima and F. Gross, A Relativistic quark model for the Omega-electromagnetic form factors, Phys. Rev. D **80**, 033004 (2009).
- [88] R. L. Workman *et al.* [Particle Data Group], Review of Particle Physics, PTEP **2022** (2022), 083C01.
- [89] G. J. Wang, R. Chen, L. Ma, X. Liu and S. L. Zhu, Magnetic moments of the hidden-charm pentaquark states, Phys. Rev. D **94**, 094018 (2016).
- [90] M. W. Li, Z. W. Liu, Z. F. Sun and R. Chen, Magnetic moments and transition magnetic moments of P_c and P_{cs} states, Phys. Rev. D **104**, 054016 (2021).
- [91] F. Gao and H. S. Li, Magnetic moments of hidden-charm strange pentaquark states*, Chin. Phys. C **46**, no.12, 123111 (2022).
- [92] F. L. Wang, H. Y. Zhou, Z. W. Liu and X. Liu, What can we learn from the electromagnetic properties of hidden-charm molecular pentaquarks with single strangeness?, Phys. Rev. D **106**, 054020 (2022).
- [93] Y. R. Liu, P. Z. Huang, W. Z. Deng, X. L. Chen and S. L. Zhu, Pentaquark magnetic moments in different models, Phys. Rev. C **69**, 035205 (2004).
- [94] P. Z. Huang, Y. R. Liu, W. Z. Deng, X. L. Chen and S. L. Zhu, Heavy pentaquarks, Phys. Rev. D **70**, 034003 (2004).
- [95] S. L. Zhu, Pentaquarks, Int. J. Mod. Phys. A **19**, 3439-3469 (2004).
- [96] A. R. Haghpayma, Magnetic Moment of the Pentaquark Θ^+ State, arXiv:hep-ph/0609253.
- [97] C. Deng and S. L. Zhu, T_{cc}^+ and its partners, Phys. Rev. D **105**, 054015 (2022).
- [98] H. Y. Zhou, F. L. Wang, Z. W. Liu and X. Liu, Probing the electromagnetic properties of the $\Sigma_c^{(*)} D^{(*)}$ -type doubly charmed molecular pentaquarks, Phys. Rev. D **106**, 034034 (2022).
- [99] F. Schlumpf, Relativistic constituent quark model of electroweak properties of baryons, Phys. Rev. D **47**, 4114 (1993); erratum: Phys. Rev. D **49**, 6246 (1994).
- [100] T. P. Cheng and L. F. Li, Why naive quark model can yield a good account of the baryon magnetic moments, Phys. Rev. Lett. **80**, 2789-2792 (1998).
- [101] P. Ha and L. Durand, Baryon magnetic moments in a QCD based quark model with loop corrections, Phys. Rev. D **58**, 093008 (1998).
- [102] R. Dhir and R. C. Verma, Magnetic Moments of ($J^P = 3/2^+$) Heavy Baryons Using Effective Mass Scheme, Eur. Phys. J. A **42**, 243-249 (2009).
- [103] A. Majethiya, B. Patel and P. C. Vinodkumar, Radiative decays of single heavy flavour baryons, Eur. Phys. J. A **42**, 213-218 (2009).

- [104] N. Sharma, H. Dahiya, P. K. Chatley and M. Gupta, Spin $\frac{1}{2}^+$, spin $\frac{3}{2}^+$ and transition magnetic moments of low lying and charmed baryons, Phys. Rev. D **81**, 073001 (2010).
- [105] N. Sharma, A. Martinez Torres, K. P. Khemchandani and H. Dahiya, Magnetic moments of the low-lying $1/2^-$ octet baryon resonances, Eur. Phys. J. A **49**, 11 (2013).
- [106] R. Dhir, C. S. Kim and R. C. Verma, Magnetic Moments of Bottom Baryons: Effective mass and Screened Charge, Phys. Rev. D **88**, 094002 (2013).
- [107] Z. Ghalenovi, A. A. Rajabi, S. x. Qin and D. H. Rischke, Ground-State Masses and Magnetic Moments of Heavy Baryons, Mod. Phys. Lett. A **29**, 1450106 (2014).
- [108] A. Girdhar, H. Dahiya and M. Randhawa, Magnetic moments of $J^P = \frac{3}{2}^+$ decuplet baryons using effective quark masses in chiral constituent quark model, Phys. Rev. D **92**, 033012 (2015).
- [109] A. Majethiya, K. Thakkar and P. C. Vinodkumar, Spectroscopy and decay properties of Σ_b, Λ_b baryons in quark-diquark model, Chin. J. Phys. **54**, 495-502 (2016).
- [110] K. Thakkar, A. Majethiya and P. C. Vinodkumar, Magnetic moments of baryons containing all heavy quarks in the quark-diquark model, Eur. Phys. J. Plus **131**, 339 (2016).
- [111] Z. Shah, K. Thakkar, A. K. Rai and P. C. Vinodkumar, Mass spectra and Regge trajectories of $\Lambda_c^+, \Sigma_c^0, \Xi_c^0$ and Ω_c^0 baryons, Chin. Phys. C **40**, 123102 (2016).
- [112] Z. Shah, K. Thakkar and A. K. Rai, Excited State Mass spectra of doubly heavy baryons Ω_{cc}, Ω_{bb} and Ω_{bc} , Eur. Phys. J. C **76**, 530 (2016).
- [113] A. Kaur, P. Gupta and A. Upadhyay, Properties of $J^P = 1/2^+$ baryon octets at low energy, PTEP **2017**, 063B02 (2017).
- [114] Z. Shah and A. Kumar Rai, Spectroscopy of the Ω_{ccb} baryon in the hypercentral constituent quark model, Chin. Phys. C **42**, 053101 (2018).
- [115] K. Gandhi, Z. Shah and A. K. Rai, Decay properties of singly charmed baryons, Eur. Phys. J. Plus **133**, 512 (2018).
- [116] H. Dahiya, Transition magnetic moments of $J^P = \frac{3}{2}^+$ decuplet to $J^P = \frac{1}{2}^+$ octet baryons in the chiral constituent quark model, Chin. Phys. C **42**, 093102 (2018).
- [117] V. Simonis, Improved predictions for magnetic moments and M1 decay widths of heavy hadrons, arXiv:1803.01809.
- [118] Z. Ghalenovi and M. Moazzen Sorkhi, Mass spectra and decay properties of Σ_b and Λ_b baryons in a quark model, Eur. Phys. J. Plus **133**, 301 (2018).
- [119] K. Gandhi and A. K. Rai, Spectrum of strange singly charmed baryons in the constituent quark model, Eur. Phys. J. Plus **135**, 213 (2020).
- [120] S. Rahmani, H. Hassanabadi and H. Sobhani, Mass and decay properties of double heavy baryons with a phenomenological potential model, Eur. Phys. J. C **80**, 312 (2020).
- [121] A. Hazra, S. Rakshit and R. Dhir, Radiative M1 transitions of heavy baryons: Effective quark mass scheme, Phys. Rev. D **104**, 053002 (2021).
- [122] C. Menapara and A. K. Rai, Spectroscopic investigation of light strange $S = -1$ Λ, Σ and $S = -2$ Ξ baryons, Chin. Phys. C **45**, 063108 (2021).
- [123] C. Menapara and A. K. Rai, Spectroscopic Study of Strangeness $= -3$ Ω^- Baryon, Chin. Phys. C **46**, 103102 (2022).
- [124] H. Mutuk, The status of Ξ_{cc}^{++} baryon: investigating quark-diquark model, Eur. Phys. J. Plus **137**, 10 (2022).
- [125] C. Menapara and A. K. Rai, Spectroscopy of Light Baryons: Δ Resonances, arXiv:2204.08840.
- [126] L. Y. Glozman and D. O. Riska, The Charm and bottom hyperons and chiral dynamics, Nucl. Phys. A **603**, 326-344 (1996); [erratum: Nucl. Phys. A **620**, 510-510 (1997)].
- [127] W. X. Zhang, H. Xu and D. Jia, Masses and magnetic moments of hadrons with one and two open heavy quarks: Heavy baryons and tetraquarks, Phys. Rev. D **104**, 114011 (2021).
- [128] T. M. Aliev, T. Barakat and M. Savci, Magnetic moments of heavy $J^P = \frac{1}{2}^+$ baryons in light cone QCD sum rules, Phys. Rev. D **91**, 116008 (2015).
- [129] B. Patel, A. K. Rai and P. C. Vinodkumar, Masses and magnetic moments of heavy flavour baryons in hyper central model, J. Phys. G **35**, 065001 (2008).
- [130] T. M. Aliev, K. Azizi and A. Ozpineci, Radiative Decays of the Heavy Flavored Baryons in Light Cone QCD Sum Rules, Phys. Rev. D **79**, 056005 (2009).
- [131] M. B. Wise, Chiral perturbation theory for hadrons containing a heavy quark, Phys. Rev. D **45**, R2188 (1992).
- [132] R. Casalbuoni, A. Deandrea, N. Di Bartolomeo, R. Gatto, F. Feruglio, and G. Nardulli, Light vector resonances in the effective chiral Lagrangian for heavy mesons, Phys. Lett. B **292**, 371 (1992).
- [133] R. Casalbuoni, A. Deandrea, N. Di Bartolomeo, R. Gatto, F. Feruglio, and G. Nardulli, Phenomenology of heavy meson chiral Lagrangians, Phys. Rep. **281**, 145 (1997).
- [134] T. M. Yan, H. Y. Cheng, C. Y. Cheung, G. L. Lin, Y. C. Lin, and H. L. Yu, Heavy quark symmetry and chiral dynamics, Phys. Rev. D **46**, 1148 (1992); [Phys. Rev. D **55**, 5851E (1997)].
- [135] M. Bando, T. Kugo and K. Yamawaki, Nonlinear Realization and Hidden Local Symmetries, Phys. Rept. **164**, 217 (1988).
- [136] M. Harada and K. Yamawaki, Hidden local symmetry at loop: A New perspective of composite gauge boson and chiral phase transition, Phys. Rept. **381**, 1 (2003).
- [137] G. J. Ding, Are $Y(4260)$ and $Z_2^*(4250)$ $D_1 D$ or $D_0 D^*$ hadronic molecules? Phys. Rev. D **79**, 014001 (2009).
- [138] R. Chen, A. Hosaka, and X. Liu, Searching for possible Ω_c -like molecular states from meson-baryon interaction, Phys. Rev. D **97**, 036016 (2018).
- [139] R. Chen, Z. F. Sun, X. Liu, and S. L. Zhu, Strong LHCb evidence supporting the existence of the hidden-charm molecular pentaquarks, Phys. Rev. D **100**, 011502 (2019).
- [140] J. Dey, V. Shevchenko, P. Volkovitsky and M. Dey, Radiative decays of S -wave charmed baryons, Phys. Lett. B **337**, 185-188 (1994).
- [141] W. J. Deng, H. Liu, L. C. Gui and X. H. Zhong, Charmonium spectrum and their electromagnetic transitions with higher multipole contributions, Phys. Rev. D **95**, no.3, 034026 (2017).
- [142] J. F. Liu and G. J. Ding, Bottomonium Spectrum with Coupled-Channel Effects, Eur. Phys. J. C **72**, 1981 (2012).
- [143] D. M. Li and S. Zhou, On the nature of the $\pi_2(1880)$, Phys. Rev. D **79**, 014014 (2009).